View Article Online
View Journal

Energy Advances

Accepted Manuscript

This article can be cited before page numbers have been issued, to do this please use: S. Mbatha, X. Cui, P. G. Panah, S. Thomas, K. Parkhomenko, A. Roger, B. Louis, R. Everson, P. Debiagi, N. Musyoka and H. W. Langmi, *Energy Adv.*, 2024, DOI: 10.1039/D4YA00433G.

ROYAL SOCIETY OF CHEMISTRY

rsc.li/energy-advances

View Article Online
DOI: 10.1039/D4YA00433G

COMPARATIVE EVALUATION OF THE POWER-TO-METHANOL PROCESS CONFIGURATIONS AND ASSESSMENT OF PROCESS FLEXIBILITY

Siphesihle Mbatha[a,c,*], Xiaoti Cui[e], Payam G. Panah[e], Sébastien Thomas[b], Ksenia Parkhomenko[b], Anne-Cécile Roger[b], Benoit Louis[b], Ray Everson[c], Paulo Debiagi[f], Nicholas Musyoka[f], Henrietta Langmi[d]

[a] *HySA Infrastructure Centre of Competence, Centre for Nanostructures and Advanced Materials (CeNAM), Chemicals Cluster, Council for Scientific and Industrial Research (CSIR), Pretoria 0001, South Africa*

[b] *Institute of Chemistry and Processes for Energy, Environment and Health (ICPEES), UMR 7515 CNRS-University of Strasbourg, 25 rue Becquerel, Strasbourg 67087 Cedex 02, France*

[c] *Centre of Excellence in Carbon Based Fuels, School of Chemical and Minerals Engineering, Faculty of Engineering, North-West University, Private Bag X6001, Potchefstroom, 2531, South Africa*

[d] *Department of Chemistry, University of Pretoria, Private Bag X20, Hatfield, 0028, South Africa*

[e] *Department of Energy, Aalborg University, Pontoppidanstr. 111, 9220 Aalborg, Denmark*

[f] *Nottingham Ningbo China Beacons of Excellence Research and Innovation Institute, University of Nottingham Ningbo China, Ningbo 315100, PR China*

*Correspondence Emails: siphe.mbatha94@gmail.com

ABSTRACT

This paper compares different power-to-methanol process configurations encompassing electrolyser, adiabatic reactor (s) and methanol purification configurations. Twelve different power-to-methanol configurations based on direct CO_2 hydrogenation with H_2 derived from H_2O-electrolysis were modelled, compared, and analysed. High temperature solid oxide electrolyser is used for hydrogen production. Fixed bed reactor is used for methanol synthesis. The aim of the paper is to give detailed comparison of the process layouts under similar conditions and select the best performing process configuration considering the overall methanol production, carbon conversion, flexibility, and energy efficiency. ASPEN PLUS® V11 is used for flowsheet modelling and the system architectures considered are the open loop systems where methanol is produced at 100 kton/annum and sold to commercial wholesale market as the final purified commodity. Further optimization requirements are established as targets for future work. Three options of power-to-methanol configuration with methanol synthesis from CO_2 hydrogenation are proposed and further evaluated considering process flexibility. From the evaluation, the series-series based configuration with three adiabatic reactors in series performed better in most parameters including the flexible load dependent energy efficiency.

Keywords: *Power-to-Methanol System Configurations, Process Design, Process Integration, Solid Oxide Electrolyser.*

View Article Online
DOI: 10.1039/D4YA00433G

1. INTRODUCTION

Investment in renewable energy has been resilient to the Covid-19 pandemic.[1] With the ongoing transition to renewable energy sources particularly variable solar and wind, and the need for cleaner fuel derivatives, chemical energy storage stands central as the best potential solution to meet these sustainability goals. Methanol is a versatile chemical intermediate and due to its ease in handling, it is a robust renewable hydrogen carrier.[2–6] Recent study by Hank et al. investigated the potential to transport renewable hydrogen using methanol, ammonia, liquid organic hydrogen carriers and methane.[3] The study reiterated the significant potential of methanol to transport large amount of green hydrogen over long distances.[3] The fact that various value-added downstream chemicals can be produced from methanol (*i.e.,* the power-to-fuels), its ease in handling and the fact that it can be used directly in the fuel cells to produce electricity (*i.e.* the power-to-power architecture) makes it attractive.

Considering plant-to-planet analysis of green methanol via using planetary boundaries tool, González-Garay et al. discovered that the potential damage that green methanol can cause to the freshwater use, nitrogen and phosphorous flow are negligible when compared to the positive effects it will have on energy imbalances, CO_2 emission reduction and ocean acidification.[7–8] According to Moioli et al. the hydrogen stored in methanol and methane processes are 85.3% and 78.2 %, respectively, thus indicating the good storage potential of methanol.[4] However, the methanol economy requires favourable policy directions.[4–6] In this front, majority of countries in the European Union (EU) as well as China have already announced ambitious plans to develop commercial scale renewable methanol plants by 2030.[5] Renewable Energy Directive II (RED II) of the EU requires that 14% of renewable energy derived fuels, including green methanol, be part of the transport sector by 2030.[9]

1.1 Recent progress in PtMeOH System level evaluation

Growing efforts are devoted to the so-called PtMeOH chain as a candidate process for sustainable methanol production via CO_2 valorisation and with hydrogen produced from renewable energy resources e.g. wind and solar via the electrolysis route.[10-16] Electrolysis technologies encompasses alkaline water-based electrolyser (AWE), polymer exchange membrane (PEM) and solid oxide electrolysers (SOEC). Numerous studies have evaluated the energetic and techno-economic feasibility of PtMeOH.[2–3, 17–24] Rivera-Tinoco et al. deduced that SOEC-based PtMeOH has a higher energy efficiency (~54.8 %) than PEM-based PtMeOH.[21] Hank et al. evaluated the transport potential, techno-economics, and energy efficiency of PEM-based PtMeOH and deduced that the process has an energy efficiency in a range of 40–44% comparable to the power-to-methane process.[3] Zhang et al. evaluated the techno-economics of SOEC-based biomass-to-methanol process and deduced that an energy efficiency of 66 % can be achieved from this process and highlighted a trade-off between the system efficiency and its production cost.[22] However, biomass-based

View Article Online
DOI: 10.1039/D4YA00433G

processes are limited by biomass feedstock availability.[20] Zhang et al. investigated the techno-economic optimization of the SOEC-based PtMeOH process and similarly observed that there is a trade-off between the energy efficiency and the production costs.[22] Bos et al. investigated the techno-economics of a 100 MW wind-based PtMeOH plant with hydrogen produced from AWE and concluded that the process has an energy efficiency of 50%.[17] Al-Kalbani et al. compared the environmental performance of fossil fuel-based and renewable energy-based PtMeOH, and their findings depicted that renewable energy-based PtMeOH is attractive from an environmental perspective.[18] The main conclusion from these studies points to high energy demands and high hydrogen production and electrolyser capital costs as the major techno-economic feasibility barriers.[3] The availability of power determines the quantity of hydrogen that can be produced and therefore the optimal capacity and system configuration.[7,17] It also emanates from these studies that the SOEC is an attractive technology from the perspective of energy efficiency and for coupling with exothermic processes such as methanol production process, although further improvements on the SOEC technology (e.g. flexibility) is still required to make its application in renewable PtMeOH more competitive.

On the other hand, these studies highlighted the required improvements in carbon capture technologies, particularly from the confines of energy penalty and costs reduction.[7,17] According to Bos et al., the methanol synthesis loop is dominated by feed compression and the key to optimizing the costs and productivity is to find the favourable ratio between the reactor size(s) and compression requirements such that the reactor operation pressure and cost of compressors remains optimized.[9, 17] The latter approach is limited by the trade-offs between pressure (i.e. feed compression duties) and conversion due to equilibrium.[7] An alternative is to reduce the recycle compression by increasing the single pass conversion, but according to González-Garay et al. and Alsuhaibani et al. this strategy has limited impact on profitability relative to decreasing the overall reactor pressure.[7, 23] Thus efforts in finding cheap and easy to scale catalysts that operates efficiently at lower pressures (<50 bar) shall not cease and their effects will become more dominant (~24.4% share of the total costs) when power-to-methanol is already economically feasible.[7] Furthermore, a combination of economically effective yield and pressure needs to be identified.[7]

It is also evident from the highlighted studies that, recently, the system level optimization has emerged as a new paradigm shift needed to improve the economics of the process.[24-29] To accelerate technology readiness and techno-economic improvement of PtMeOH, several demonstration projects have been implemented and some are being planned.[26] Nonetheless, availability of data from demonstrated systems remains scarce and difficult to access. On the other hand, modelling efforts in this direction have thus far been directed to a single objective or only two objectives i.e. energy efficiency and production costs. Thus, optimized process flowsheets that enhances the CO_2 and H_2 conversions, energy efficiency, process economic (lowering production costs and/or capital), flexibility and reduce CO_2 emissions and system

View Article Online
DOI: 10.1039/D4YA00433G

complexity are required.[3] Due to low conversion of the direct CO_2 hydrogenation over the $Cu/ZnO/Al_2O_3$, GhasemiKafrudi et al. optimised the process recycle flow to improve the performance.[24] They considered different process parameters, including temperature, pressure, and GHSV, to reduce the recycle, energy consumption and greenhouse gas emissions of the CO_2 hydrogenation process. Furthermore, GhasemiKafrudi et al., investigated the effect of changes in the hydrogen injection as make up gas, applying two reactors, inert gases, moisture in the feed, the use of dry hydrogen and the recycle stream on methanol yield.[24] Their results showed that having two reactors with intermediate dehumidification in series and adding hydrogen as make-up at the inlet of the second reactor increases the methanol yield by a factor of 1.8.[27] However, the authors also deduced that if one reactor with recycle is used, the resultant methanol yield is almost double when compared to the case of one reactor with no recycle.[24] Finally, GhasemiKafrudi et al., concluded that by just modifying the catalyst type and total amount (decrease slightly e.g. in their case; total amount =865kg) and increasing the inlet temperature (e.g. in their case to 209 °C), the recycle flow reduces by almost 38%.[24] Moioli et al. and Lee et al. have already established that for a CO_2 hydrogenation on $Cu/ZnO/Al_2O_3$ based catalyst, and for both small scale and commercial scale (~100 kton/annum), three cascade fixed-bed reactors are optimal.[4,14] Lee et al. deduced that a configuration with three reactors in series, having intermediate cooling and separation of methanol/H_2O between the reactors is optimal in-terms of profit (from a deficit of \$4.3 to \$2.5 profit per ton) and CO_2 conversion (~52%).[14] However, Lee et al. using a process superstructure and techno-economic optimization methods investigated the best configuration that optimizes the profit for the two step CO_2 hydrogenation process in which both CO_2 and CO participate as carbon sources in hydrogenation reactions to methanol and focusing only on the synthesis and purification step instead of the direct CO_2 hydrogenation process as will be considered in this study.[14] Furthermore, the superstructure optimisation approach tends to discard the suboptimal flowsheets following set objectives and constraints without giving further details as to why the suboptimal process underperforms and the possibility of improving it further.[27]

More recently, Chiou et al. investigated six different configurations for the PtMeOH focusing on single stage and multistage series reactor(s) connections with adiabatic and non-adiabatic (with co-current cooling) reactor type.[28] Their study focused on design, optimisation, control, techno-economics, and environmental aspects of the process considering a small scale (20 kton/y) plant capacity. They reached the conclusion that two reactors with first stage non-adiabatic (with co-current cooling) and second stage adiabatic reactor type in series with inter-stage cooling and separation of methanol and water was more economically attractive (with a minimum selling price of methanol of 998US\$/ton and carbon tax of 283US\$/ton) and showed better performance. From this, they devised a control strategy aimed at handling the throughput and compositional disturbances for their proposed configuration. The rejection of two kinds of compositional disturbances i.e. (i) the 5% N_2 and (ii) the H_2 impurity were investigated. Their control

View Article Online
DOI: 10.1039/D4YA00433G

strategy allowed the rejection of both compositional disturbances within 5h. It was noted that increases in N_2 impurity composition deteriorates the reaction kinetics and increases the purge rate which reduces methanol production rate with higher loss of CO_2 and H_2. Thus, to maintain the single pass conversion, H/C ratio will have to be increased. The authors however did not investigate any full integrated process with electrolyser, parallel-series configuration, and the three-stage reactors with intercooling, nor the detailed load change flexibility of their system.

1.2. Recent progress in PtMeOH process flexibility

Production processes are prone to stochastic variation for example in system input parameters, internal process parameters and environmental factors.[30] A degree of process flexibility helps to deal with these challenges. The level of process flexibility affects the economic gain of the process and the selection of the right conditions (i.e. parameters, location, capacity, etc.) in which the process operates economically.[30-33] In this paper, flexibility refers to the ability to handle the changes in the feedstock composition/flow or adjustments to other changing boundary conditions in order to adapt the plant operation to the changes in the energy or material supply.[34] It is well-known that the electrolyser, in particular the PEM type which is suitable for rapid start-up, can provide good flexibility.[32,35-36] Lange et al. recently gave a good technical review of the state of the art of the electrolyser technology's flexibility including the SOEC technology which will be considered in this study due to its high efficiency.[36] Lange et al. deduced that the SOEC can provide a broad range of load flexibility (-100% to 100 %), but this is countered by its long cold-startup time (~60min).[36] However, efforts are being made on the front of improving the performance of the materials for the SOEC cells/stack to allow more flexibility and shorten the start-up time without incurring severe cell damage.[36-37] The recent results such as in the work of Li et al. showed great potential of the future of the SOEC in handling flexibly the intermittent renewable energy supply with reduced start-up time.[37]

In a coupled electrolysis-methanol synthesis system, intermediate gas (hydrogen and CO_2) storage under intermittent conditions may be needed unless the reactor operates flexible. If the reactor has a wide tolerance to variations in the operational parameters, it is referred to as the load flexible reactor. The load range of the catalytic reactor is a function of chemical reactions, transport rate, catalysts, and reactor design.[32] The attainable load flexibility of the methanol reactor section has not been investigated, at-least intensively.[31-33] At the present, to the author's knowledge, only INERATEC Gmbh has expressed interest to investigate and scale-up the flexible modular micro-structured reactors. Considering the case of variable renewable energy-based processes, flexibility is typically achieved by over-sizing the main process equipment to account for variability in the load. The size of the equipment directly influences the propagation of disturbances within the unit and the bigger the size, the smaller the influence of disturbances on process

View Article Online
DOI: 10.1039/D4YA00433G

variables. However, the load range of the reactor is also limited by operational issues such as maximum temperature rise and ability to achieve autothermic control i.e. in which the reactor outlet is used to heat the feed (via feed-effluent heat exchanger concept).[31] The heat of reaction is, with careful heat management, generally enough to heat the feed to the methanol synthesis reactor(s) and/or distillation column, thus allowing the system to operate autothermally i.e. achieving energy self-sufficiency without external heating/cooling. In cases where the reactor feed stream is not sufficiently heated, the reaction rate will decrease and thus rendering low outlet temperature, which in effect results into lower inlet temperature and consequently the reaction halts completely. According to the study on fixed bed reactors performed by Zimmermann et al., with methane as an example, the step responses typically implemented by switching from one steady-state to another were found to be the worst-case load change policy due to the existence of unfavourable behaviour such as temperature overshoot and conversion drops.[38] Proper design of the network structure can help achieve necessary flexibility without additional oversizing of the equipment.[39] According to Grossmann & Morari, flexibility cannot be simply achieved by ad hoc addition of equipment or oversizing but by systematic design techniques.[40]

Rinaldi & Visconti assessed the steady state and transient performances of a multi–tubular fixed bed reactor for methanol production from biogas.[41] Their modelled system had a methanol synthesis reactor, a flash unit, and accounted for the unconverted gas recycle. The novelty of their conceptual work was to assess the possibility to run a multi–tubular methanol synthesis reactor flexibly, i.e., using the carbon dioxide from biogas and renewable H_2 in order to increase methanol productivity when the process is economically feasible. In their work, the investigation of the methanol synthesis multi–tubular reactor is conducted considering the impacts, on methanol productivity, temperature profile and transient behavior, of the two operating conditions i.e. (i) when the cost of green hydrogen is high, the excess of CO_2 in the biogas is vented and the reactor is fed with CO_2-lean syngas only; (ii) conversely, when affordable renewable H_2 is available, CO_2 is co-fed into the reactor along with this affordable green H_2.[41] These authors compared a 1D and 2D model in terms of its ability to better predict the temperature and production profile.[41] They deduced that the concerned reactor manages well both operating conditions with steady state reached within a few hours when switching from one condition to another and that 2D model are better suited to predict the temperature and methanol production profile. Moreover, they also highlighted that reducing the number of tubes (equivalent to the reducing catalyst amount and measured using GHSV) instead of the reactor length is preferred especially for small scale processes. Reducing the length of the reactor can lead to unacceptable hot-spots from the resultant worsening of the convective heat transfer and reduced selectivity to methanol. When the length of the reactor is shortened, the thermal peak is achieved at higher temperatures, and the gaseous stream remains mostly in the kinetic regime to near the end of the reactor.[41]

View Article Online
DOI: 10.1039/D4YA00433G

This was prevalent when syngas is fed with and without co-feeding the CO_2 and H_2, and when the length of the reactor was decreased below half (up to ¼) of the original length.[41]

Furthermore, Svitnič and Sundmacher investigated the effect of flexibility of the methanol synthesis process on the levelized cost of methanol (LCOM).[42] In their finding, the flexibility gains are most prominent for the designs with a single source of renewable energy (either solar or wind) leading to reduction of costs of more than 10%. This gain is significantly reduced for the design with combined solar and wind resources, as the complementary availability of renewable resources allows to better sustain stable operation of the chemical processes, reducing the influence of flexibility to 5.1%. Moreover, the authors deduced that the flexible operation of the methanol synthesis has a stronger effect on the reduction of LCOM, where for the design with a single renewable resource it delivers a roughly 4-times larger reduction of LCOM.

More recently, Qi et al. investigated different strategies for flexible operation of the power-to-X processes coupled with renewables using PtMeOH as a reference.[33] The strategies they compared involved the use of the energy buffers i.e. the hydrogen intermediate storage, liquid CO_2 energy storage as a Carnot battery, and Li-ion battery storages. In considering the latter they generated nine process configurations with islanded, grid-assisted only, and grid-assisted bidirectional connections for allocation of energy. Qi et al. considered a combination of solar and wind energy as well as grid electricity purchase.[33] The configurations with grid-assisted bidirectional connections resulted into the most cost-effective way for flexible operation of the power-to-X and the lowest levelized cost (~479.4 US$/ton) was achieved when the Carnot battery was used. However, this is still more expensive than the methanol produced from autothermal reforming of natural gas which can reach a cost of 285.6US$/ton and thus indicating that further research and development is needed to make renewable methanol production cost-competitive with other methods. In addition, some trade-offs were observed amongst the performance indexes which indicate that there is no single best solution but rather more case dependent solutions. Moreover, studies are required that incorporate the dynamic modelling of the energy buffer and the electrolyser to account for the factors such as the time varying energy efficiency and the limitations on power ramp-up.[33] Process operation can influence the design of the process and hence the flowsheet. Compared to investigations focusing on methanol synthesis catalyst improvements, studies focusing on PtMeOH reactor design, process configurations and process flexibility are very few. The objective of this paper is to model and compare different PtMeOH process layouts under steady state and dynamic conditions with the consideration of their process flexibilities.

1.3 Statement of originality

The originality of the work in this paper lies in the comparative flexibility analysis of different integrated methanol synthesis system configurations comprising parallel-series and series-series connections. Twelve

View Article Online
DOI: 10.1039/D4YA00433G

integrated flowsheets (including co-electrolysis and the electrified reverse water gas shift (e-RWGS) system) based on SOEC, methanol synthesis and purification steps are contrasted to assess their performance in terms of energy efficiency, production rate, and material conversion. In addition, the better performing CO_2 hydrogenation-based flowsheets are assessed under dynamic mode for their flexibility and to answer the following questions:

1) What is the feasible (with minimum sophisticated equipment) load-change flexibility window?
2) What is the effect of the load change in the parallel-series and series-series-based configurations?
3) How do the energy efficiency and conversion in the mentioned flowsheets design changes with the change in the load?

Candidate PtMeOH configuration(s) with methanol synthesis from CO_2 hydrogenation is proposed. Furthermore, optimization requirements are established as targets for future work. The paper is structured as follows: Section 2 gives the base content and approach to modelling, Section 3 gives the detailed results and discussion, Section 4 concludes the work and Section 5 give recommendations for future work.

2. PROCESS SYNTHESIS AND MODELLING

Twelve different flowsheets are synthesized and simulated (see section 2.2.2 table 6 and supplementary material section A2 for more details) under steady state conditions in Aspen Plus® V11 and out of the twelve, three are selected for flexibility assessment under Aspen Dynamics V11 platform. Table 1 shows the assumptions pertaining feed conditions. The system's capacity is designed to store about 162 MW of renewable electricity from either wind or Solar PV farm. This is in scale of a commercial size plant.[43-45] For all flowsheets, the SOEC configuration was left unchanged, however the methanol synthesis section configuration was modified to generate twelve different process configurations. Following the findings of Samimi et al. on the possibility to enhance the production rate of methanol with exclusion of inert in the feed, inert are thus neglected in this study.[46]

Table 1: Feed conditions.

Raw materials	Temperature(°C)	Pressure (bar)	Flowrate (kmol/hr)	Composition (mol %)
CO_2	25	1.0	401	100
H_2O	25	1.0	1232	100
Sweep gas (oxygen)	25	1.0	31	100
Steam electrolysis product H_2 feed stream to MEOH unit				
H_2	35	5.0	1212.5	98.8
H_2O	35	5.0	14.3	1.2
Co-electrolysis product syngas feed stream to MeOH unit				
H_2	35	5.0	1212.5	74.3
CO_2	35	5.0	105	6.4
CO	35	5.0	296	18.1
H_2O	35	5.0	19.3	1.2

View Article Online
DOI: 10.1039/D4YA00433G

The exclusion of inert allows setting the lowest possible purge as detected by the system control parameters.[9, 47] Recycle ratio is an effective control parameter of the process (particularly the reactor) productivity and temperature.[46] It is also critical to highlight that the dynamic modelling of the SOEC to ascertain its capability is beyond the scope of this work. Rather the focus on dynamic modelling is placed on the downstream reactor configurations to establish their flexibility.

2.1 SOEC modelling

The electrochemical model to simulate the SOEC was implemented in ASPEN PLUS® V11 in the FORTRAN routine with the use of design specifications and calculator functions. Water, sweep–gas (oxygen) and electricity are the primary feeds to the SOEC unit. The thermodynamic model used in modelling the electrolysis is the Redlich-Kwong Soave equation of state (EOS) with modified Huron-Vidal mixing rules (RKSMHV2).[48-50] The main electrochemical model is a function of product species, which are electrochemically active i.e. i=H_2. The net voltage is expressed by equation 1 below:

$$\mathrm{E_i} = E_{nerst,\,i} + {E_{act,i}}^{her} + {E_{act,\,i}}^{oer} + E_{ohm,\,i} + E_{mic,\,i} \quad (1)$$

Where $E_{nerst,\,i}$ is the Nernst potential, $E_{act,i}$ refers to the over-potential due to activation of electrochemical reactions, $E_{ohm,\,i}$ refers to the ohmic over-potential and $E_{mic,\,i}$ is the interconnect voltage losses. The system is assumed to operate at thermoneutral stack voltage and under steady state, thus equation 2 is used as the main equation to calculate the thermoneutral energy.

$$\mathrm{E_{tn}} = \frac{\Delta H_r}{I_{tot}} = \mathrm{E_i} \quad (2)$$

Where ΔH_r is the heat of reaction, and I_{tot} refers to the total current (A). According to Giannoulidis et al. it is advantageous from the perspective of the SOEC energy efficiency to operate the unit at low pressure (<10 bar).[2] For the selected operating conditions, thermoneutral operation is achievable.[45, 51] Generally, the planar O-SOEC is operated in the temperature range of 150 °C – 950 °C and pressure range of 1–8 bar.[2,52–53] The SOEC operating under co-electrolysis conditions can already produce syngas at ratio of 1.5 to 3.5.[53] The SOEC unit capacity is designed for 109 MW considering the SOEC operating under steam electrolysis only. However, for the co-electrolysis based SOEC unit capacity only 134 MW is required to produce the syngas given in Table 2. Table 2 shows the input parameters used in the modelling of the SOEC unit. Generally operating the SOEC at higher temperature lowers the electricity requirements and hence increases the energy efficiency. The choice of temperature is a reasonable compromise between allowable concentration over-potential, ohmic over-potential and possibility of achieving thermo-neutral point operation.

View Article Online
DOI: 10.1039/D4YA00433G

Table 2: SOEC operating conditions and parameters for steam and co-electrolysis

Parameter	Value	Unit
Steam inlet temperature of SOEC	850	°C
Air inlet temperature of the SOEC reactor	850	°C
SOEC stack temperature	850	°C
Reactant utilization	70	%
H_2 cathode inlet recycle	10	%
Operation pressure	5.0	bar
Stack consumption	29.7	kWh/kgH_2
Hydrogen production	2827	kg/h
Syngas production	15360	kg/h
Syngas ratio (methanol feed)	2.2	-
LHV of syngas	25	MJ/kg

Typically, near or at thermoneutral point, high electrolysis efficiency and minimum sweep gas flowrate are achievable.[2] This makes operating the electrolyser at thermoneutral point attractive.[2,54–55] Figure 1 illustrates the SOEC model flowsheet for steam electrolysis implemented in ASPEN PLUS. Figure 2 illustrates the SOEC model flowsheet for co-electrolysis implemented in ASPEN PLUS. For steam electrolysis (see Figure 1), demineralized water (stream WATER) is first pumped to increase its pressure to SOEC operating pressure, then vaporised and superheated in a cascade of heat exchangers, and mixed (via CATHOD-M) with cathode feed recirculation (i.e. stream H_2-Recycle stream) which contains 10 mol% of hydrogen.[56-60] The fraction hydrogen is recycled to prevent electrode (i.e. Ni-YSZ) re-oxidation.[56] The composition of steam in the SOEC feed (i.e. stream SOEC-FEE) is maintained above 90% to prevent starvation at the electrode, which may cause cell damages. The SOEC cathode is modelled using RSTOIC, using the conditions in Table 2 and the feed steam utilization factor (i.e. in the SOEC-C unit) is assumed to be 70%. The product stream (i.e. stream PRODUCT-1) containing oxygen, hydrogen and unconverted water of the SOEC cathode (SOEC-C) is separated in the electrolyte (i.e. ELECTROL) into PRODUCT-2 and PRODUCT-3. Stream PRODUCT-3 contains only water and hydrogen, and it is split (i.e. SPLIT) into product stream containing wet hydrogen (i.e. stream PROD-4) and recycle stream (i.e. H2-RECYC). Stream PROD-4 is used to pre-heat the feed stream, and it is ultimately cooled and fed to the separator block (i.e. WATER-SEP) in which a significant quantity of water (i.e. stream WWATER) is removed (discharged or recycled) and wet hydrogen at 98.8 mol% is fed to the methanol synthesis section. Stream PRODUCT-2 contains only oxygen. The cascade heat exchanger network is used to recuperate the heat from the effluent streams for the purpose of generating superheated steam at cheaper cost. Sweep gas (i.e. stream SWEEP-GA) is assumed to contain only oxygen and is first compressed (via COMP-1) to SOEC pressure, heated (via FEHE 2, HEATER 2) to SOEC temperature and fed to anode side (i.e. modelled as ANODE-M) of the SOEC unit to remove the oxygen produced during electrolysis. The removed oxygen is then used in the cascade heat exchangers to preheat steam, after which it is then cooled and expanded to atmospheric conditions before being discharged or alternatively sold or sent to another process (i.e. stream O2-DISCH).

View Article Online
DOI: 10.1039/D4YA00433G

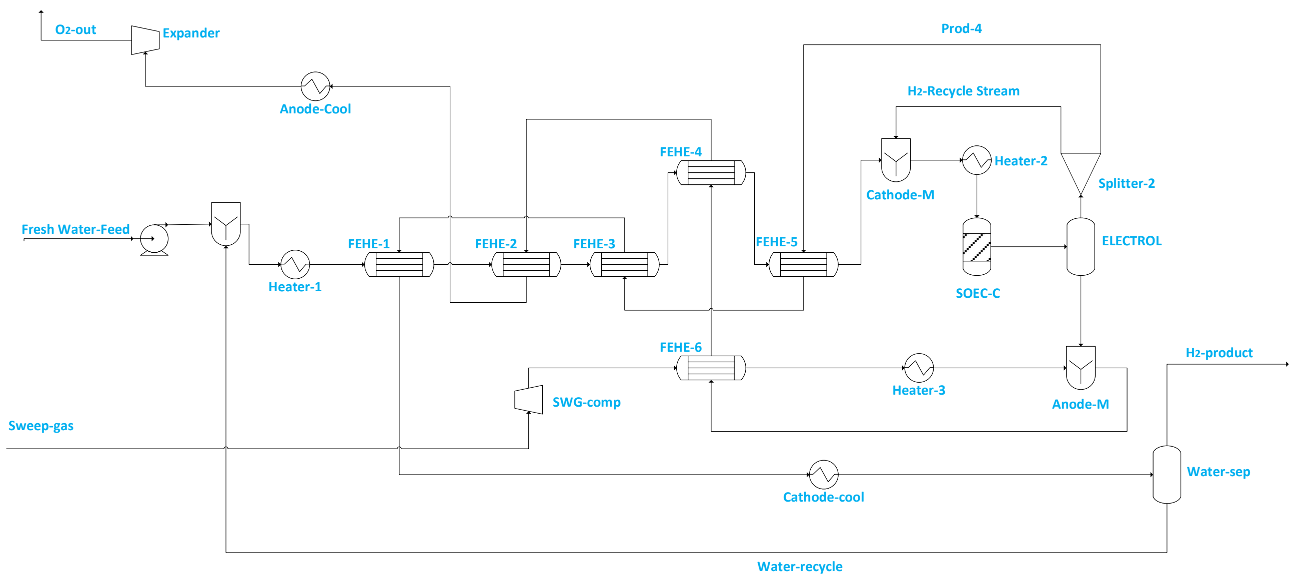

Figure 1 Illustration of the SOEC unit used for steam electrolysis in ASPEN PLUS®.

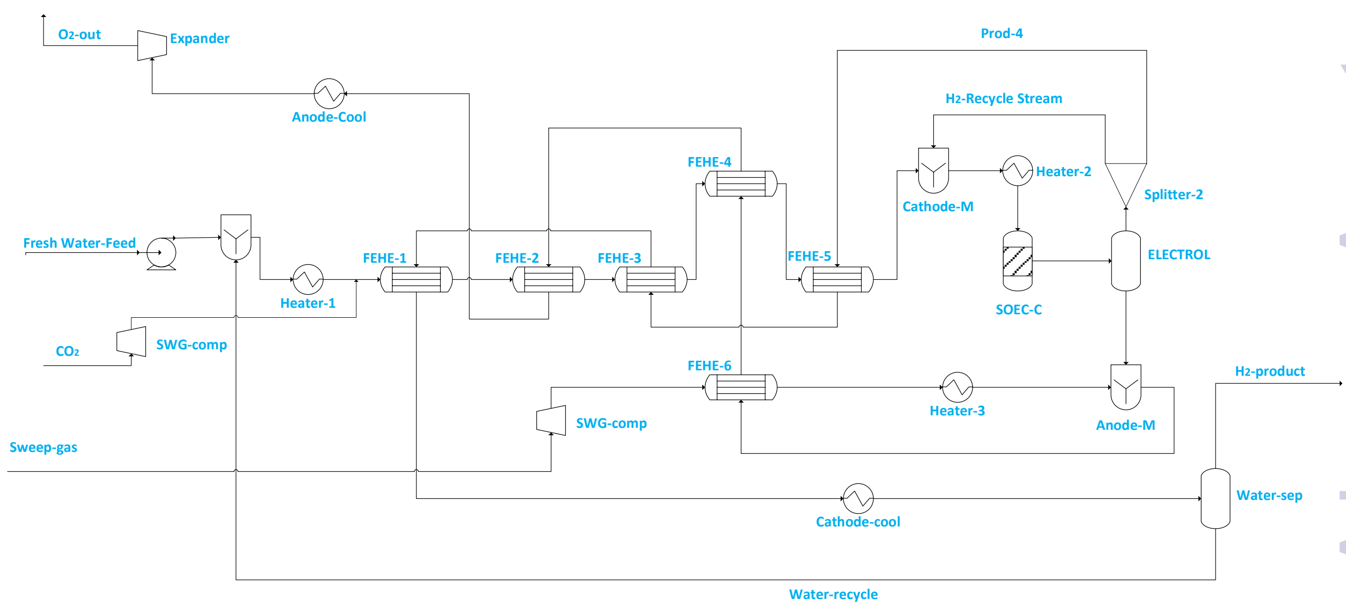

Figure 2 Illustration of the SOEC unit used for co-electrolysis in ASPEN PLUS®.

The use of oxygen (recirculated) as a sweep gas manages possible overshoot in the over-potential; therefore allows for higher energy efficiency operation of the electrolyser. During the start of the process, oxygen is assumed to come from its storage tank, while during operation it can be recirculated from the anode with some stored or sold to end users. It is noted beforehand that the use of oxygen may increase the exergy destruction, but the difference between the exergy efficiency when steam or air is used as sweep gas is expected to be marginal, with steam as sweep gas having the exergy efficiency which is ~1% more than that of oxygen.[47,57] In addition, using oxygen as a sweep gas allows the production of pure oxygen which can be sold to market.[47, 57]

View Article Online
DOI: 10.1039/D4YA00433G

2.2 Steady state: reactors and separation modelling

Both CO_2 and H_2 feed streams are compressed to 78 bar using multiple compressors each with an isentropic efficiency of 75% for the steam electrolysis-based PtMeOH. For the co-electrolysis-based system, the syngas feed is compressed in a two-stage compression system to 78 bar with same isentropic efficiency. Considering safety aspects as it would be necessary in real plants, the compression ratio is kept at 3 and inter-stage cooling is included. The temperature of the feed stream to reactor(s) was set to 210 °C.[61] The inlet temperature is in a typical range of an optimised industrial methanol reactor[61], a higher inlet temperature can result in a higher outlet temperature and a lower methanol yield, particularly for the adiabatic reactor(s). In addition, the lower limit for allowable inlet temperature is defined by the catalyst, and for the commercial copper-based catalyst it is around 190 °C.[62] Commercial $Cu/ZnO/Al_2O_3$ catalyst is used in this study. Reactor (s) is modelled as an adiabatic reactor(s). Table 3 gives the properties of adiabatic reactor(s) modelled as a plug-flow (RPLUG) and those related to the catalyst. Adiabatic reactors have lower cost relative to the water-cooled and gas-cooled reactors due to their simple structural designs.[62] The advantage of adiabatic reactors is that under nominal steady state conditions their size is very small, thus their over-sizing slightly affect the capital cost.[63-65] This indicates their potential in small scale PtMeOH processes as well.[62] The reactor size was selected to be large enough such that the effluent from the reactor is near equilibrium.[47] Redlich-Kwong-Soave equation of state with modified Huron-Vidal mixing rules (RKSMHV2) was used to model the reactor(s), auxiliaries and to calculate the thermodynamic properties of the streams (refer to Section A1 of the Supplementary Material). After separation of methanol and water using a flash drum, a recycle stream was then purged up to 0.1% for all flowsheets (see section A4.2 of the supplementary material for the sensitivity on recycle fraction). In line with the work of Cui *et al*., the small purge of 0.1% was set, which aims to minimize the CO_2 emission for the green methanol production.[66] As observed from Cui et al. using a larger purge ratio can result in lower flow rate of the recycle stream as well as a smaller reactor size but a higher CO_2 loss. It was also observed from Cui et al. that a value lower than 0.1% may cause convergence problem.[66] For the syngas (co-electrolysis-based system), the purge stream after methanol separation and recycle was set to 1.3%.

Table 3: Adiabatic plug-flow reactor (s) operating conditions

Parameter	Value	Unit
Tube diameter	3-5	m
Tube length	3-12	m
Reactor inlet pressure	74-75.7	bar
Catalyst particle density	1775	kg/m^3
Bed porosity	0.5	-
GHSV	4000-7300	h^{-1}

View Article Online
DOI: 10.1039/D4YA00433G

2.2.1. Reaction kinetics

Industrially, methanol is synthesized from syngas following the three main equilibrium reactions as expressed by equations 3-5 over an industrial $Cu/ZnO/Al_2O_3$ catalyst. However, it is has been recently agreed and demonstrated that methanol can also be produced from a feed with pure CO_2/H_2 i.e., via equation 3 only even though the actual reaction mechanism and carbon source for methanol remains an active subject of debate.[10–13]

$$CO_2 + 3H_2 \leftrightarrow CH_3OH + H_2O \qquad \Delta H_{298K} = -49.43 kJ/mol \qquad (3)$$

$$CO_2 + H_2 \leftrightarrow CO + H_2O \qquad \Delta H_{298K} = +41.12\ kJ/mol \qquad (4)$$

$$CO + 2H_2 \leftrightarrow CH_3OH \qquad \Delta H_{298K} = -90.55\ kJ/mol \qquad (5)$$

Following Le'Chaterliers principle, higher methanol yields are favoured at lower temperatures and higher pressures. However, for the reason of enhancing kinetics, temperatures in the range of temperature 200–300 °C are used as well as high pressure ranges of 50-100 bar over the commercial $Cu/ZnO/Al_2O_3$ catalyst. The reverse water gas shift reaction (equation 4) is the only endothermic reaction in the three main reactions and therefore gets promoted as temperature increases. This reaction increases the amount of water generated in the case when pure CO_2/H_2 is the main feed. This lowers the selectivity to methanol and the catalyst activity. As a result, significant research efforts are devoted to the CO_2 hydrogenation to methanol process, mostly to improve the catalyst conversion and selectivity.[14–15] However, the commercial $Cu/ZnO/Al_2O_3$-based catalyst is likely to remain the best possible for some time due to its ability to achieve highest yield, its low costs, and high stability.[16] Ruland et al. established, through dynamic experimental conditions relevant to power-to-methanol (PtMeOH), that the industrial $Cu/ZnO/Al_2O_3$ is highly stable for conditions of chemical energy storage with hydrogen produced from fluctuating renewable energy sources, indicating its relevance for application in PtMeOH.[16] Besides the challenges of optimizing the catalyst beyond what the commercially available catalyst can achieve to promote CO_2/H_2 to methanol, this reaction is attractive from an environmental perspective in that a significant quantity of CO_2 can be recycled, and in addition it is less exothermic, thus rendering ease of heat management in the reactor, and fewer by-products formation. For these reasons and following the most recent kinetic analysis such as in the work of Nestler et al, Slotboom et al., and de Oliveira Campos et al., who deduced that the role of CO hydrogenation to methanol is negligible at high CO_2/CO feed ratio, in this work and only reactions 3 and 4 are considered in the modelling of the methanol synthesis.[67-69]

The kinetic model used in this study was presented in the work of Van-Dal & Bouallou.[64] which originated initially from the model of Bussche and Froment.[63, 65] The model assumes methanol production from CO_2 hydrogenation (i.e., equation 2) in the presence of RWGS as a competing reaction (equation 4) and absence

View Article Online
DOI: 10.1039/D4YA00433G

of diffusional limitations. Thus, the effectiveness factor equals 1. The kinetic model is based on Langmuir Hinshelwood Hougen-Watson (LHHW) kinetic model formulation and is expressed by equations 6 and 7.

$$r_{CH_3OH} = \frac{k_1 P_{CO_2} P_{H_2} - k_6 P_{H_2O} P_{CH_3OH} P_{H_2}^{-2}}{\left(1 + k_2 P_{H_2O} P_{H_2}^{-1} + k_3 P_{H_2}^{0.5} + k_4 P_{H_2O}\right)^3} \left[\frac{kmol}{kg_{cat} s}\right] \quad (6)$$

$$r_{RWGS} = \frac{k_5 P_{CO_2} - k_7 P_{H_2O} P_{CO} P_{H_2}^{-1}}{1 + k_2 P_{H_2O} P_{H_2}^{-1} + k_3 P_{H_2}^{0.5} + k_4 P_{H_2O}} \left[\frac{kmol}{kg_{cat} s}\right] \quad (7)$$

Where k_i were calculated for implementation in ASPEN PLUS V11® using the equation 8 and these are tabulated in Table 4 below.

$$\ln k_i = A_i + \frac{B_i}{T} \quad (8)$$

Table 5 presents the main parameters of the distillation column which was modelled as RadFrac in ASPEN PLUS V11®.

All flowsheets used the same conditions, except only the distillation (DC) in flowsheet 2 in which the boilup ratio was set to 0.9 (lower) to ensure the methanol purity remains above 99wt%. NRTL-RK was selected as a property method to model the distillation column and its feed (with pressure ≤1.1bar).

Table 4: Kinetic parameters rearranged for implementation in ASPEN PLUS V11® as a LHHW model.[54,57]

Kinetic parameters	Ai	Bi
k_1	-29.87	4811.2
k_2	8.147	0
k_3	-6.452	2068.4
k_4	-34.95	14928.9
k_5	4.804	-11797.5
k_6	17.55	-2249.8
k_7	0.1310	-7023.5

Table 5: Main parameters of the distillation column used for final separation of methanol.

Parameter	Value	Unit/basis
Column	RadFrac	-
Number of trays	30	-
Condenser type	Partial-Vapor-Liquid	-
Reflux ratio	1.5-1.62	mole
Boilup ratio	0.9- 1.5	mole
Feeding temperature	80	°C
Operating pressure	1.1	bar

Validation of the kinetic model is presented in the supplementary material section A2. The typical catalyst pellets of 6mm×4mm was packed in the catalyst bed and Ergun equation was used for pressure drop calculation through the catalyst bed. Following process engineering principles, the reactors were sized at

View Article Online
DOI: 10.1039/D4YA00433G

constant total reactor(s) volume. A hold-up time of 5 minutes was used in sizing the separators, and the compressor curves were used to model the compressors. Valves were modelled taking into consideration the typical efficiency relations and pressure drops. Thus, in modelling the different systems, the following summary of assumptions were made:

- An adiabatic fixed-bed tubular reactor has been used to convert CO_2 and H_2 into methanol. The overall CO_2, H_2O or H_2 feed is kept constant as in Table 1.
- The kinetics model and its parameters are kept constant. Where there are multiple reactors, the total reactor volume of all the reactors combined is kept constant similar to base case flowsheet 1 with one reactor as shown in the Supplementary Material section A3, Figure S3 and Section A5, Table S10. This keeps constant the total amount of catalyst used in all flowsheets, which is paramount for cost effective comparison.
- The reactor feed temperature is selected in the optimal temperature range (210<Tin<240) to optimise the temperature profile and conversion in the reactor.[62] Refer to the section A4 (sensitivity-based optimisation) of the Supplementary Material.
- The by-products are negligible, and thus the produced materials in the reactor are methanol, CO, and water.
- Solar PV is used as a source of electricity. In the process, the water is used for cooling.
- Catalyst deactivation is negligible.
- The temperature of any flow or equipment is not considered lower than 20 °C, so that there is no need for a refrigerant cycle.
- The operating conditions have been selected with respect to the limitations of the industrial equipment and considering the outcomes of the design sensitivity analysis in section A4 of the supplementary material.
- In the hydrogen stream entering the process, 1.2 mol percent of water are considered.

2.2.2 System Configurations

It is important to highlight all flowsheet comprises a recycle loop, and the SOEC flowsheet was fixed for better comparison. Flowsheet 1 to 6B are shown in the supplementary material section A3 along with their brief description. To be concise, in this section, only the finally selected flowsheet 7, 7B and flowsheet 8 are shown as these will be discussed in more details in the subsequent sections. Table 6 gives the description of the different flowsheets. The selection follows from the comparison with flowsheet 1 to 6B as described in the results section 3. Flowsheet 7 illustrated in Figure 3 includes two reactors connected in parallel followed by intermediate separation of methanol and series connection with the third reactor and thereafter, recovery of methanol from the recycle using two separators and a further separation of residual gases at

View Article Online
DOI: 10.1039/D4YA00433G

low pressure before the distillation column from which the final methanol product flows. Flowsheet 7B illustrated in Figure 4 has almost similar components as flowsheet 7 but the difference is that all reactors are connected in series. Flowsheet 8 illustrated in Figure 5 has three reactors connected in series, but the flowsheet is simplified series connection version of flowsheet 7B.

Table 6: Description of different flowsheets, their advantages, and limitations.

Process configuration	Description	Advantages	Limitations
Flowsheet 1	This is the base configuration with a single stage adiabatic reactor.	• Simple configuration. • Less equipment and thus capital investment. • Simple start-up process.	• Large recycle stream is required for this process. • Low single pass conversion. • More valuable hydrogen purged.
Flowsheet 2	Single stage reactor, with stripper column mounted before the reactor to enhance condensation and separation of methanol from CO_2 and remove water from the wet hydrogen feed.	• Help to prevent catalyst deactivation from wet hydrogen. • Enhances the separation of dissolved gases from the methanol/water mixture.	• Large recycle stream is required for this process. • Low single pass conversion. • More valuable hydrogen purged.
Flowsheet 3	Comprises two adiabatic reactors in series and with intermediate cooling and separation of methanol and water at 45 bar and 35°C. The other feature of flowsheet 3 is the addition of compressor to the feed of the second reactor to raise the operating pressure of the second reactor to the same pressure as the first reactor in the scheme.	• Optimises the pressure to the second reactor and the overall pressure profile to enhance methanol production on the second reactor. • Enhances the conversion of the unconverted gases from the first stage. • Reduces the recycle stream.	• Increase number of equipment means more capital investment. • Repeated heating and cooling.
Flowsheet 4	It has two reactors in series but with a wash column which uses $C_3H_8O_3$ as a solvent mounted in the position after the reactor followed by separation and two distillation columns in which the first is used for solvent recovery while the second distillation column is used for methanol purification.	• This design enhances the driving force of the reaction by eliminating as much as possible the water and methanol from the unconverted gases. • Enhances the conversion of the unconverted gases from the first stage. • Reduces the recycle and compression work.	• Increase number of equipment means more capital investment. • Increased pressure drop with more reactors, and slightly increased compression. • Complexity and additional solvent recovery requirements. • Repeated heating and cooling.
Flowsheet 5	Closely resembles flowsheet 3 with two reactors in series but with a change in operation of the intermediate separator which is operated at pressure equal to the reactor pressure to avoid the compression of the feed to the second reactor which comprises unconverted gases and some fraction of methanol.	• Reduces compression work and recycle. • Enhances the conversion of the unconverted gases from the first stage.	• Increase number of equipment means more capital investment. • Increased pressure drop with more reactors, and slightly increased compression.
Flowsheet 6A	Has two reactors connected in parallel. It also has long recycle to both reactors and therefore a feed (comprising fresh feed and recycle) split at 50% to both reactors.	• Increases the residence time in each reactor and thus aims at enhancing the conversion. • Reduces the number of intermediate separators. • Reduces repeated heating and cooling.	• High recycle flowrate. • High compression requirements.
Flowsheet 6B	Has two reactors connected in parallel. It has a short recycle in which the fresh feed flow is split to 50% and the portion of the fresh feed to the second reactor in flowsheet 6B is mixed with all the recycle of unconverted gases whereas the portion to the first reactor is kept as fresh feed.	• Increases the residence time in first reactor and thus aims at enhancing the conversion. • Reduces the number of intermediate separators.	• High recycle flowrate • Relatively poor overall conversion. • Removes the recycle as a lever for temperature control in the first reactor especially for part-load operation.
Flowsheet 7	Includes two reactors connected in parallel followed by intermediate separation of methanol and series connection with the third reactor and thereafter, recovery of methanol from the recycle using two separators and a further separation of residual gases at low	• Increased reactants conversion and flexible loading/operation. • Reduced compression requirements, and hence potentially improved energy efficiency.	• Increase number of equipment means more capital investment. • Increased pressure drop with more reactors, and slightly increased compression requirement.

View Article Online
DOI: 10.1039/D4YA00433G

Process configuration	Description	Advantages	Limitations
	pressure before the distillation column from which the final methanol product flows.	• Reduced purge stream and hence CO_2 emissions.	• Complex start-up and shutdown with repeated heating and cooling.
Flowsheet 7B	Has almost similar components as flowsheet 7 but the difference is that all reactors are connected in series. The feed to the third reactor is taken from the overall recycle stream and compressed further to boost the pressure.	• Increased reactants conversion. • Reduced compression requirements, and hence potentially improved energy efficiency. • Reduced purge stream and hence CO_2 emissions.	• Increase number of equipment means more capital investment. • Increased pressure drop with more reactors, and slightly increased compression requirement. • Complex start-up and shutdown with repeated heating and cooling.
Flowsheet 8	Has three reactors connected in series, but the flowsheet is a simplified series connection version of flowsheet 7B. This configuration has no booster compressor for the feed to all downstream reactors except the main recycle compressor feed.	• Increased reactants conversion. • Reduced compression requirements, and hence potentially improved energy efficiency. • Reduced purge stream and hence CO_2 emissions.	• Increase number of equipment means more capital investment. • Increased pressure drop with more reactors, and slightly increased compression requirement. • Complex start-up and shutdown with repeated heating and cooling.
Co-electrolysis flowsheet	Has three reactors connected in series, similar to flowsheet 8. The main difference is the upstream steam-electrolysis step which is replaced to co-electrolysis and thus leading to fresh feed to the reactor with syngas instead and increased CO concentration.	• Existing catalyst optimised for the syngas feed. • Co-electrolysis step enhances the energy efficiency of system. • Enhanced conversion with the introduction of CO.	• Would practically results in the more impurities and difficulties in downstream separation as the existing industrial syngas systems. • Selectivity to methanol decreases with increase in CO/CO_2 ratio.
e-RWGS flowsheet.	Has three reactors connected in series, similar to flowsheet 8. The main difference is the upstream steam electrolysis step which is coupled e-RWGS and thus leading to fresh feed to the reactor with syngas instead, and increased CO concentration.	• Enhanced conversion with introduction of CO. • Existing catalyst optimised for the syngas feed. • Higher CO/CO_2 ratio leads to higher methanol production.	• Would practically results in the more impurities and difficulties in downstream separation as the existing industrial syngas systems. • Selectivity to methanol decreases with increase in CO/CO_2 ratio. • Required separation of water formed from e-RWGS reactor.

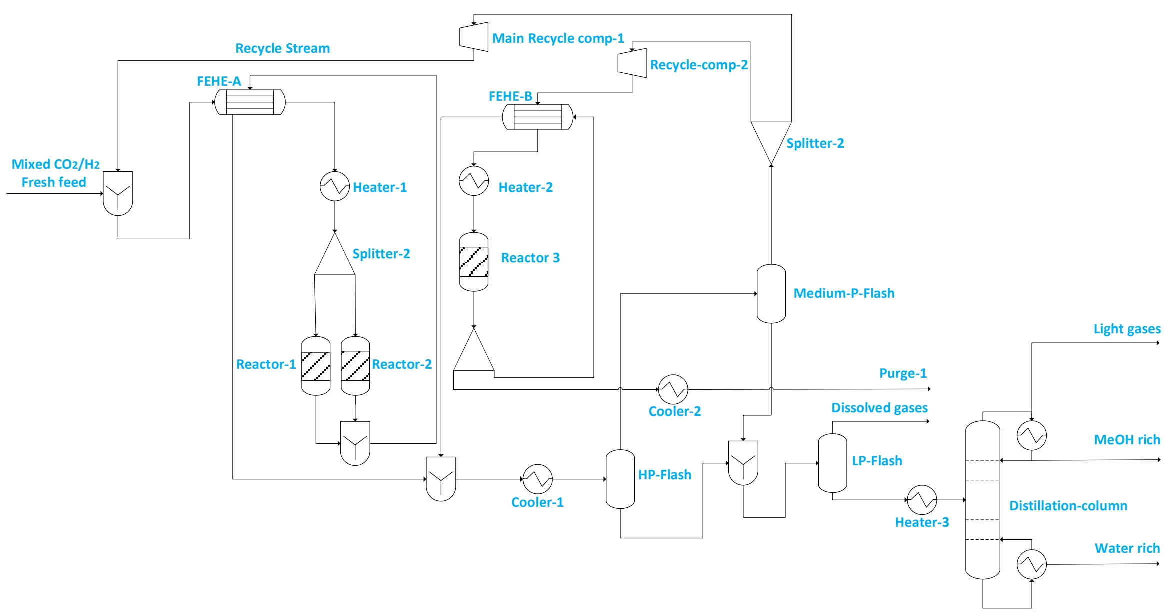

Figure 3: Illustration of Flowsheet 7. This flowsheet features parallel-series configuration of the three adiabatic reactors.

View Article Online
DOI: 10.1039/D4YA00433G

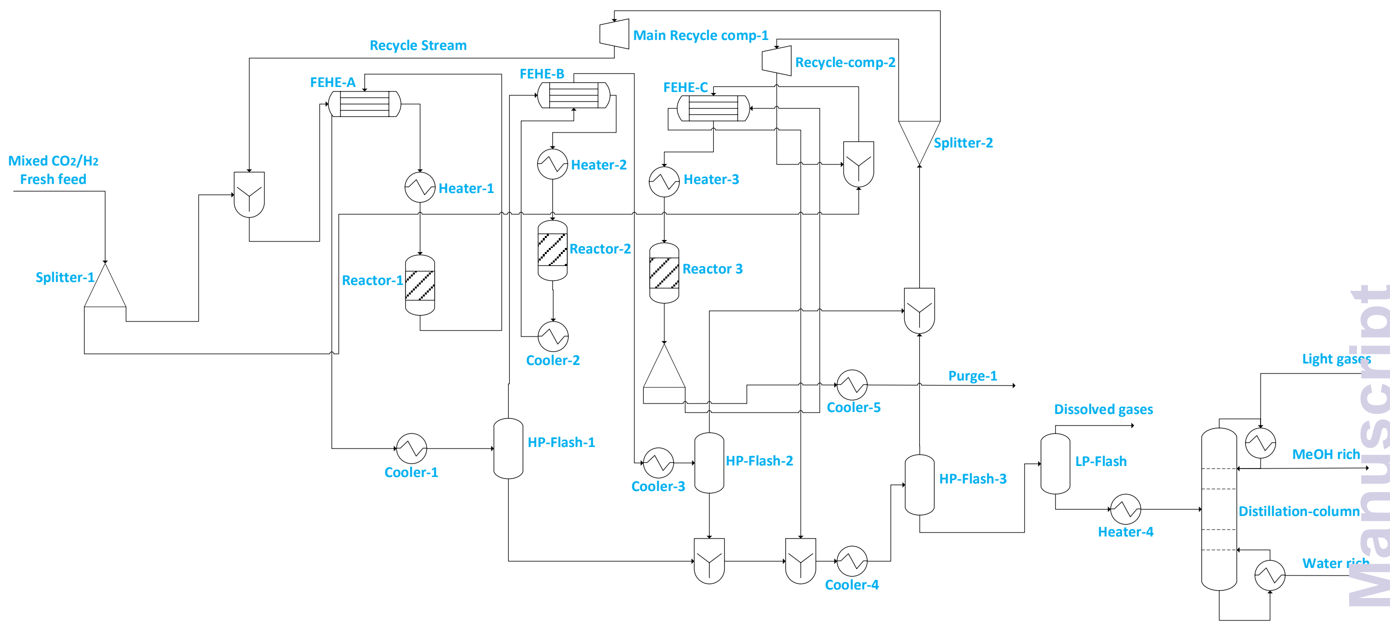

Figure 4: Illustration of Flowsheet 7B. This flowsheet features three reactors in series with intermediate cooling. This features a different feed, product-purge arrangement to the third reactor (reactor 3).

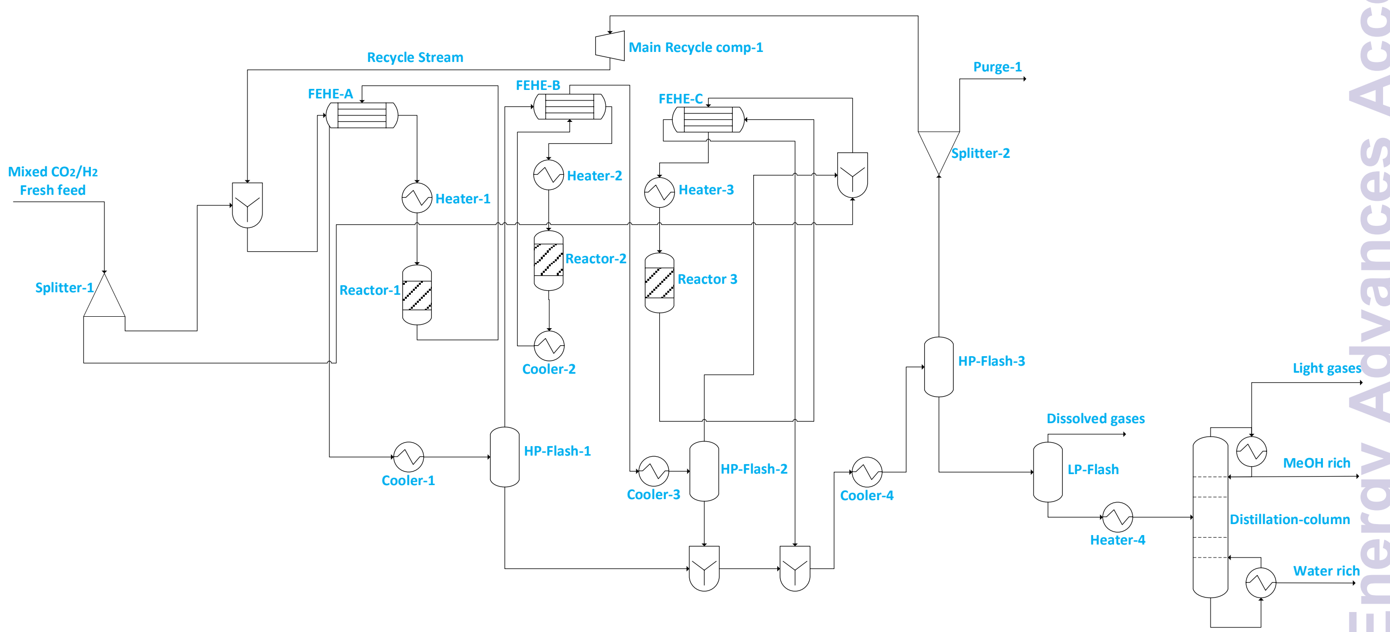

Figure 5: Illustration of Flowsheet 8. This flowsheet features three adiabatic reactors in series with intermediate cooling.

2.3 Dynamic reactors system modelling for flexibility analysis

Three of the most promising reactor configurations were selected and assessed in comparison for their flexibility analysis. The loads were varied from minimum to maximum (i.e., 40-102%) with consideration

View Article Online
DOI: 10.1039/D4YA00433G

of practicality in the design of the equipment such as pumps, compressors (e.g., to prevent surge and stonewall), etc. Dynamic modelling of the methanol synthesis section is conducted using the ASPEN DYNAMICS V11®. The initial state of the different reactor configurations were extracted from steady-state simulations conducted using Aspen Plus by means of pressure driven approach leading to a more realistic model comparable to real plants. The flowsheets after dynamic translations (with all critical control loops) are shown in the supplementary material, section A4.1. The dynamics of the process are highly dependent on the reaction kinetics and modelling approaches.[34] For the dynamic simulation, the distillation section is excluded following the findings from Cui et al. that distillation dynamics, which affects the product quality, is easy to manage under variable loads.[66] For the methanol synthesis, the feed H_2 and CO_2 were mixed at stoichiometric ratio of H_2/CO_2 =3, before being mixed further with the recycle stream.

Signal generators were used during the dynamic modelling, to alter the rates of flow change (i.e., load change) for the feed gases. Moreover, tuned proportional–integral (PI) controllers were used for dynamic operation. The proportional and integral gains were tuned based on the Ziegler-Nichols and Tyreus-Luyben tuning rules by using the automatic controller tuning in ASPEN DYNAMICS V11®. Details of the tuned controllers are shown in the supplementary material. The systems are evaluated considering the KPIs such as energy efficiency, flowrate of the feed streams (i.e., load change), reactor conversion, heat duties and power of the compressors. The hydrogen produced from the renewable electricity and methanol represents the major power input and output, respectively.

2.4 Technical performance indicators

The mass and energy balance of the process configurations were calculated. The selected indicators to evaluate the studied processes including the overall CO_2 conversion, energy efficiency, production rate, and load change are used as criteria for comparisons. The energy efficiency expressions of the SOEC system, and the overall system defined below, follows from the work of Lonis et al. and Cui et al.[59–60, 66] For the SOEC unit operating to produce hydrogen or syngas as the key product, equation 9 describe the expression for the efficiency the water electrolysis section.

$$\%\eta_{SOEC,\,product} = \frac{\dot{m}_{product} \times LHV_{product}}{P_{SOEC} + P_{BOP,SOEC}} \tag{9}$$

Where $\dot{m}_{product}$ refers to the mass flowrate of hydrogen or syngas (for co-electrolysis), $LHV_{product}$ refers to the lower heating value of hydrogen or syngas, P_{SOEC} refers to the electric power of the SOEC while $P_{BOP,SOEC}$ is the power of the SOEC auxiliaries. Single pass conversion of carbon is expressed by equation 10. The CO is considered in the calculation of single pass conversion since the feed to the reactor contains CO introduced by recycle although the overall system boundary feed to the process doesn't contain CO but

View Article Online
DOI: 10.1039/D4YA00433G

only CO_2 and H_2O. The efficiency of the integrated SOEC and the methanol synthesis i.e., the PtMeOH efficiency can be described using equation 11.

$$\%\eta_{C,\,conversion} = \frac{(CO_{2,\,in}+CO_{in})-(CO_{2,\,out}+CO_{out})}{(CO_{2,in}+CO_{in})} \tag{10}$$

$$\%\eta_{PtMeoH} = \frac{\dot{m}_{MeOH}\times LHV_{MeOH}}{P_{SOEC}+P_{BOP,SOEC}+E_{MSS}+P_{BOP,\,MSS}} \tag{11}$$

Where E_{MSS} refers to the heat energy requirements in the methanol synthesis unit (MSS) i.e., for preheating the feed to the reactor and distillation column, and for reboiler in the distillation. The $\dot{m}_{MeOH}$ (kg/h) is the mass flow rate of the streams, *LHV* is the lower heating value for the gases, and *P* represents the heat duty of the heat exchangers or the power inputs for the recycle compressor and pumps. Furthermore, heat integration is also considered for all the most promising flowsheets and thus the composite curves and exchanger designs are investigated. Heat integration eliminates/reduces external heat requirements in the methanol synthesis and distillation section (i.e., yield to E_{MSS} ≈0). A brief analysis of the impact of heat integration on the three selected flowsheets (flowsheet 7, 7B and 8) is presented in section A4.3 of the Supplementary material.

3. RESULTS AND DISCUSSION

3.1 Electrolyser performance: steam vs co-electrolysis

Table 7 summarises the energy balance pertaining the heating and cooling within the SOEC system. High temperature SOEC) has an advantage in terms of having higher energy efficiency. This is because this technology utilises both heat and electricity. In general, the higher the temperature the lower the electricity demand. On the other hand, increasing the temperature reduces the overvoltage losses i.e., the ohmic losses. Therefore, the SOEC exhausts (anode and cathode) are used to preheat and superheat the feed streams containing recirculated oxygen sweep gas and demineralized water.

Table 7: Energy balance in the SOEC section under steam electrolysis.

Heating process	**Heat (kW)**	**T_{in} (°C)**	**T_{out} (°C)**	**Cooling process**	**Heat (kW)**	**T_{in} (°C)**	**T_{out} (°C)**
Sweep air PH by heat recovery (FEHE6)	116	248	650	Anode exhaust 1st cooling (FEHE6)	-113	850	831
Sweep air SH by external source (Heater3)	61	650	850	Anode exhaust 2nd cooling (FEHE4)	-1273	831	619
Water PH and VAP external heat (Heater1)	21602	28	180	Anode exhaust 3rd cooling (FEHE2)	-137	619	595
Water SH by heat recovery (FEHE1)	2422	180	332	Anode exhaust 4thcooling (ANOD-COOL)	-2587	595	130
Water SH by heat recovery (FEHE2)	137	332	340	Cathode exhaust 1st cooling (FEHE5)	2110	850	707
Water SH by heat recovery (FEHE3)	2755	340	505	Cathode exhaust 2nd cooling (FEHE3)	-2755	707	515
Steam SH by heat recovery (FEHE4)	1273	505	579	Cathode exhaust 3rd cooling (FEHE1)	-2422	515	342
Water SH by heat recovery (FEHE5)	2111	579	697	Cathode exhaust 1st cooling (CAT-COOL)	-9023	342	35
Steam SH by external heat (Heater 2)	2835	714	850				

SH=super heat, VAP=vaporisation, PH=preheating

View Article Online
DOI: 10.1039/D4YA00433G

Additional external heat source is still required to preheat and vaporise demineralized water, and further raise the temperature of the demineralized steam and sweep gas to the SOEC operating temperature (850 °C). Table 8 summarises the performance of the steam and co-electrolyser considering the power consumption and energy efficiency. The steam electrolysis-based SOEC required to produce about 1213 kmol/h of hydrogen under the operating conditions stipulated in Table 2, a corresponding electrical power of approximately 109 MW is required. Since the electrolyser is operated at thermoneutral voltage, the efficiency is high due to negligible overpotential losses compared to endothermic operation.[55] The steam-based SOEC system efficiency value of $\eta_{soec,system}$ = 74.5%-78.2% obtained in this work is comparable to values that have been reported in literature for the SOEC efficiency values [52-53, 55-56] at thermoneutral voltage such as the value ($\eta_{soec,sytem}$ = 83 %) which was presented in the work of Lonis et al. who used the definition of energy efficiency similar to equation 9 above, even though the model for SOEC was fairly simplified in this work.[60] The slight under-estimation of efficiency in this work is perhaps due to the differences in model formulation. However, the results are very comparable to what literature reports for SOEC energy efficiency at thermoneutral voltage[52-53, 55-56] and thus giving confidence about the relevance of model formulation assumptions in this work. On the other hand, the co-electrolysis based SOEC efficiency considering the BOP energy consumption was found to be around $\eta_{soec,\ system}$ = 76–79% and comparable to literature.[32, 55] The power consumption in co-electrolysis mode is however higher than that in the steam based SOEC mode and this trend is similar to that found by Patcharavorachot et al. [50] This is because in co-electrolysis mode, both H_2O and CO_2 conversion reactions consume electrical power.[50]

Table 8: Performance of the electrolyser system for steam electrolysis and co-electrolysis

		Steam-electrolysis	Co-electrolysis
Parameter/index	**Units**	**Value**	**Value**
LHV (H_2 or CO+H2)	MJ/kg	120	25
Psoec	MW	84	107
Psoec,BOP	MW	25	27
$\eta_{soec,\ system}$	%	74.5	76.2
$\eta_{soec,\ system,\ R}$	%	78.2	79.2

However, for the co-electrolysis-based mode, a slightly higher (1.7% more than water-electrolysis mode) overall SOEC system energy efficiency was obtained for the same ratio. This is mainly due to reduced feed steam requirements in co-electrolysis mode, as part of the steam is produced from CO_2 to CO reaction (i.e., RWGS). It is also critical to highlight that the hot streams from the SOEC have been used only for the heating of the cold streams in the SOEC section to avoid complications of the process and to better assess the influence of the configured methanol synthesis section on the overall energy efficiency of the process. This renders the two system thermally independent, which is advantageous when variable renewable

View Article Online
DOI: 10.1039/D4YA00433G

electricity is used in PtMeOH, provided this is achieved at minimal possible cost. This allows for some degree of flexible part-load operation for each section with reduced regulation or operation issues.

As also highlighted by Chen and Yang et al., integration of heat between two or more subsystems should be minimized unless otherwise necessary, and optimal integration (also reducing heat curtailments) within a subsystem should be maximised.[31] For the final heating of the steam via heater 3, an external source is required (e.g. electricity) in order to achieve the operating conditions of the SOEC. An alternative would be to operate the electrolyser above thermoneutral point and thus use the surplus heat from overpotentials, but this is not considered in this study as it adversely promotes cell degradation. External electrical heat requirements for the SOEC section (≈24% of the total electrolysis power) is needed to generate superheated steam and heat the sweep gas to the SOEC temperature. The sweep gas must first be compressed and heated to the SOEC temperature.

3.2 Methanol Production Rate, Energy Efficiency, Overall and Single-pass CO_2 and H_2 Conversion

Comparison of the process flowsheet configurations based on methanol production rate, energy efficiency, carbon conversion and H_2 conversions are shown in Figure 6, Table 9 and 10. The overall CO_2 conversion is calculated considering a recycling system in all configurations. Comparison of the methanol production rate shows that three reactors, gives higher methanol production rate. The highest methanol production rate is found for flowsheet 7B which comprises of three reactors in series with intermediate cooling and separation. Comparison of the process flowsheets (see Figure 6) depicts that configuration expressed as flowsheet 5 has a slightly higher energy efficiency. Flowsheet 7B has a similar overall CO_2 and H_2 conversion and energy efficiency as flowsheet 7 and flowsheet 8. However, the flowsheet 7B differs slightly (about 1% less) in terms of the energy efficiency compared to flowsheet 5. Table 9 shows the single pass CO_2 conversion of each reactor per flowsheet configuration. Since the process configuration of flowsheet 1 and 2 follows from the work of Van-Dal & Bouallou and Kiss et al. the single pass CO_2 conversion from this work are comparable to those of Van-Dal & Bouallou and Kiss et al. for flowsheet 1 and 2, respectively.[54,58, 63] The reason the flowsheets 1 and 2 were re-modelled in this work was to ensure fair comparison using similar scale and process conditions since the original work of Van-Dal and Bouallou and Kiss et al. used distinct conditions and/or target production capacities and kinetics.[61, 64, 70] Even if the capacities were to be similar, different operating conditions will yield different performance. Single pass conversion in series reactors with intermediate cooling shows an increasing trend as reactor stages increase. This is so as the removal of water and methanol via intermediate cooling and separation increases the driving force of the CO_2 conversion reaction and thus enhances CO_2 conversion. Although flowsheet 2 can produce a high methanol comparable to flowsheet 7, 7B and 8, it has a slightly lower energy efficiency.

View Article Online
DOI: 10.1039/D4YA00433G

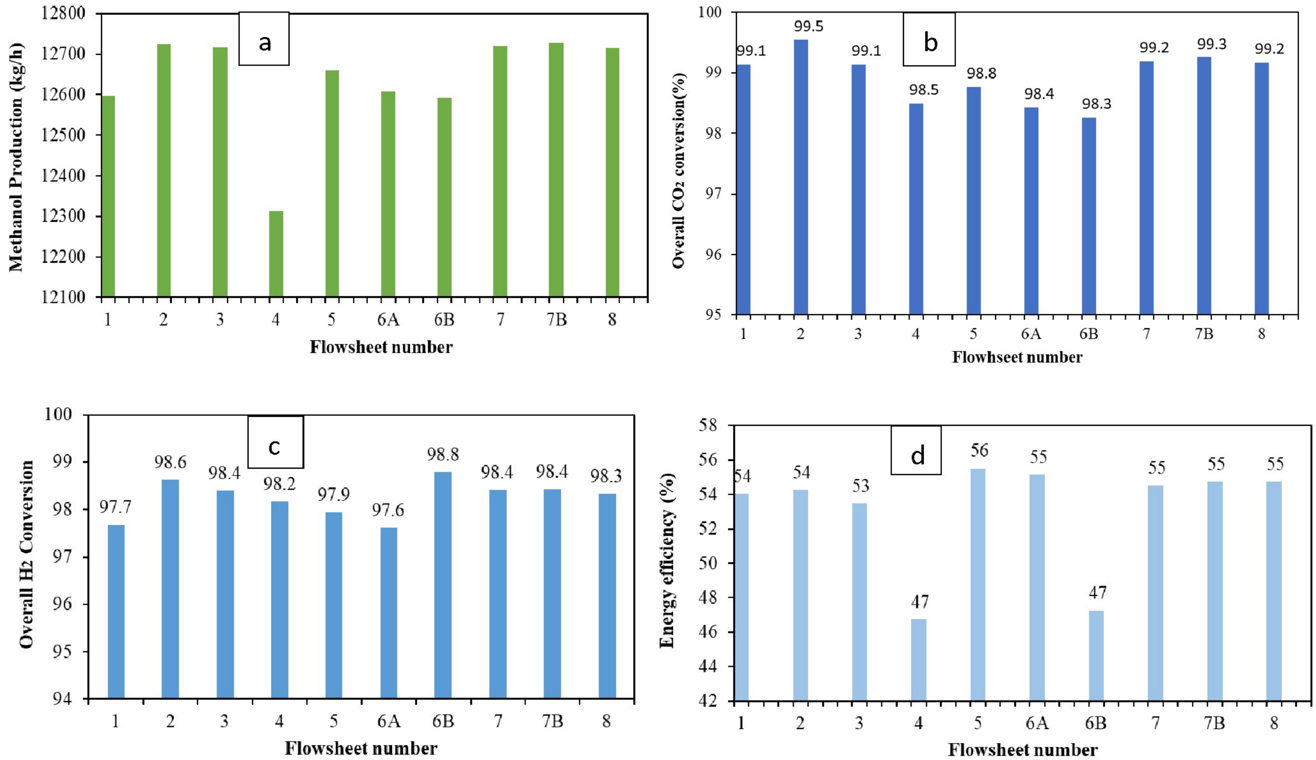

Figure 6: Performance of the different flowsheet considered in this paper: (a) methanol production. (b) overall CO_2 conversion. (c) Overall H_2 conversion. (d) Overall energy efficiency of the process.

Table 9: Single pass carbon conversions of each reactor in the evaluated process configurations.

	Flowsheet number									
	1	2	3	4	5	6A	6B	7	7B	8
Reactor (R)	% CO_2 Conversion in each reactor in the flowsheet									
R1	39.1	17.8	39.7	39.0	40.4	42.0	47.4	51.5	32.8	30.3
R2	-	-	53.6	53.9	55.8	42.0	10.1	51.5	42.8	40.3
R3	-	-	-	-	-	-	-	34.5	50.2	46.6

Table 10: Single pass H_2 conversions of each reactor in the evaluated process configurations.

	H_2 % conversion per flowsheet number per reactor									
	1	2	3	4	5	6A	6B	7	7B	8
R1	9.3	18.6	8.6	9.2	9.2	9.2	8.1	7.0	11.1	11.2
R2	-	-	6.7	7.0	6.5	9.2	4.3	7.0	9.6	10.0
R3	-	-	-	-	-	-	-	10.2	7.6	7.5

View Article Online
DOI: 10.1039/D4YA00433G

Despite effort to recover as much methanol in flowsheet 4 with additional separation via solvent wash column, the overall methanol production and energy efficiency is not improved for this process. This is because thermodynamically limits on recoverable methanol in a given stream. This process may also introduce losses of valuable reactants that may otherwise be recycled and reconverted. For parallel reactors having a short recycle stream, similar to configuration in Flowsheet 6B, slightly decreases the overall methanol production rate and CO_2 conversion. The short recycle also results in large recycle stream and hence increased recycle compressor duty. This decreases the energy efficiency and hence flowsheet 6B has low energy efficiency as indicated in Figure 6d. When these parallel reactors are designed with a long recycle (flowsheet 6A) and equally divided feed each reactor has a single pass conversion slightly higher than flowsheet 1 & flowsheet 2 which is expected because a smaller mole flowrate of the reactants is fed for comparable catalyst mass inside these reactors, thus resulting into higher residence time and hence increased carbon conversion.

Table 11: Comparison of the energy efficiency obtained from this study and those found in literature.

Reference	**Energy efficiency (%) w/o heat integration**
Hank et al. [12]	40.2-44.1
Rivera Tinoco et al. [14]	54.8
Szima & Cormos [71]	53.93
Bos et al. [15]	50
Parigi et al. [72]	58.8
This study	Flowsheet 5: 56 Flowsheet 7: 55 Flowsheet 7B: 55 Flowsheet 8: 55

The trend of conversion with changes in flowrate is also observable when reactors are staged in series with intermediate cooling. The rapid increase in the conversion of R3 corresponding to Flowsheet 7B is a result of significant reduction in its feed flow-rate since the series staging of the reactors converts more of the reactants (overall, each reactor in the earlier stages receive higher flows) and the subsequent intermediate segregation of methanol and water which increase the driving force on reactor R3. In addition, the analysed process conversion is higher due to absence of impurities in the feed. The results are comparable to the findings of Basonde & Urakawa, who experimentally demonstrated the similar single pass CO_2 conversion using 10:1 H_2/CO_2 feed.[73] The performance that would be achieved with 3.333 times more hydrogen (expensive to make from electrolysis) than the stoichiometric ratio in the feed is the same as having the configurations as discussed with the H_2/CO_2 of 3:1 in the overall feed. Thus, the reactor configuration strongly influences the conversion of CO_2 to methanol.

Hydrogen storage is another key goal of the PtMeOH process. In this regard, the storage of hydrogen is assessed in terms of the amount of hydrogen that is converted to methanol in the process. Viewed from the

View Article Online
DOI: 10.1039/D4YA00433G

overall process-based hydrogen conversion as depicted in Figure 6, methanol production using flowsheet 6B with short recycle had a higher overall H_2 conversion. This is achieved without application of hydrogen gas recovery, e.g. membranes, which are often applied industrially to increase the overall conversion of hydrogen. The use of membrane was not considered in this paper due to it potential to increase the methanol production cost. Table 10 shows the single pass conversion of hydrogen to methanol. The single pass conversions of hydrogen are lower than the CO_2 single pass conversions since hydrogen is always in excess in the feed of the reactor due to a significant amount of it in the recycle.

Figure 6 also plots the energy efficiency of the flowsheets. The trend without heat integration shows that flowsheet 5 has the highest energy efficiency followed by flowsheet 7, 7B and 8. However the production rate of flowsheet 5 is slightly lower than those of flowsheet 7, 7B and 8. This is because flowsheet 7, 7B and 8 have the additional reactor which converts more materials and thus have a slightly higher production rate. This shows a trade-off between the energy efficiency and the production rate. As the production rate increases energy efficiency decreases slightly. For flowsheet 5, the intermediate flash drums for separation of methanol and water from unconverted gases are operated at high pressures. This in effect reduces the energy requirements and size of the compressors to the second reactor and recycle. This depicts a trade-off between compression cost and flash drum pressure as observed by Luyben et al.[9] This implies that caution must be taken to avoid increasing pressure excessively in a way that the contents of unconverted gases and inert in the liquid stream sent to the distillation column increases (thus reducing the quality of the product) or significantly reducing the pressure and thus increasing the compression requirements of the recycle compressor. The flowsheet 7, 7B and 8 have the same energy efficiency (see Table 11). Thus, this indicate a trade-off, between production rate and energy requirements which has been articulated by several other authors.[22, 56] However, looking at the temperature profile at the exit of the reactor in flowsheet 7, 7B, 8 opportunities for heat integration exists and could improve the energy efficiency of the process. Mechanical work and process heating (excluding the integrated heating) in this work are powered by electricity only. Energy efficiencies are still low, and this indicates the need to perform heat integration analysis and heat exchanger network design which is summarily performed and discussed in section A4.3 of the supplementary material. Before performing heat integration, sensitivity-based optimisation of the reactor section of the flowsheets is investigated for flowsheet 7, 7B and 8 to determine the optimal operating conditions associated. The result of the design sensitivity are shown in section A4.2 of the supplementary material. Sensitivity on critical parameters such as the recycle ratio, fresh feed partitioning, feed temperature reactor, separator pressure and temperature were performed. The findings shows that fresh feed partitioning does not change the methanol production rate but can influence the control of the hot spot temperature and offer a degree of freedom under dynamic operation. From the heat integration, the series-series configuration showed low utility requirements upon optimisation of the heat exchanger network.

View Article Online
DOI: 10.1039/D4YA00433G

3.3 Assessment of flexibility of the methanol synthesis section

3.3.1 Feed flowrate and product streams

Generally, reactor configurations influence the flexibility of the process.[32] In this section, both parallel-series and series-series based configuration are assessed. Both series- and parallel-series-based configurations with three reactors are modelled under dynamic conditions by changing the load (feed flowrate). Simultaneous modulation of the CO_2 and H_2 feed is performed to maintain the CO_2:H_2 ratio of 1:3 in the feed. In a cascade series-series reactor design (i.e., flowsheet 7B, 8 and syngas-based flowsheet), changes in the conversion and temperature in one stage influences the reaction rate of the next stage. The non-linear relationship of temperature and concentration may render some intermediate load points infeasible, even though the minimum and maximum may be feasible. However, this was found to not be the case for all the four designs considered in the present study. The minimum and maximum loads used in this study are $\beta_{min} = 40\%$ and $\beta_{max} = 105\%$ for flowsheet 7, 7B and 8. While the syngas-based flowsheets had the minimum allowable load-change of 45% of the nominal. Below these β_{min} values, the Aspen Dynamics integrator fails. The part-load refers to 50% of nominal load. In this study, a load ramp (R) of 60% load per hour and a total time on stream of 15 hours were considered. Figure 7 shows effect of load change from full-load to part-load on flowrates of the main feed and product streams. A linear decrease in the flowrate from full-load to part-load occurs during t=1—2.19 h and linear from full-load to part-load increase from t=5—9.51 h is depicted. This is desirable as it promises quick and good response to process variability under intermittent renewable energy. As expected, following the previous study on a single reactor by Cui et al. both the methanol production rate and the purge stream follows the same trend of the load change.[66]

All three configurations had the relatively comparable process flexibility; meaning they all achieved/tolerated minimum to full load operation without any violation of path constraints such as maximum allowable temperature in the reactors. However, it took 1.08, 1.16 and 1.19 h to reach the part-load steady state for flowsheets 7, 7B and 8, respectively. To reach the full load steady state from the part-load conditions, it took 1.51, 3.21 and 4.51 h for flowsheet 7, 7B and 8, respectively. Small undershoots and overshoots are observed on the purge stream for all flowsheet at minimum load. Although these flowsheets can handle the load change very well, parallel-series configuration (flowsheet 7) seems to be attractive with the ability to reach steady state faster. For all flowsheets, dual control (split range control) of the recycle split ratio (see flowsheets details on the supplementary material) was necessary to reach low load levels and hence dynamize the methanol synthesis section. In Figure 7B, there is an overshoot in the purge after part-load operation and it took longer than 24 hours for the purge in this flowsheet to stabilise to the initial steady state value. When comparing the CO_2 hydrogenation-based flowsheet to the syngas-

View Article Online
DOI: 10.1039/D4YA00433G

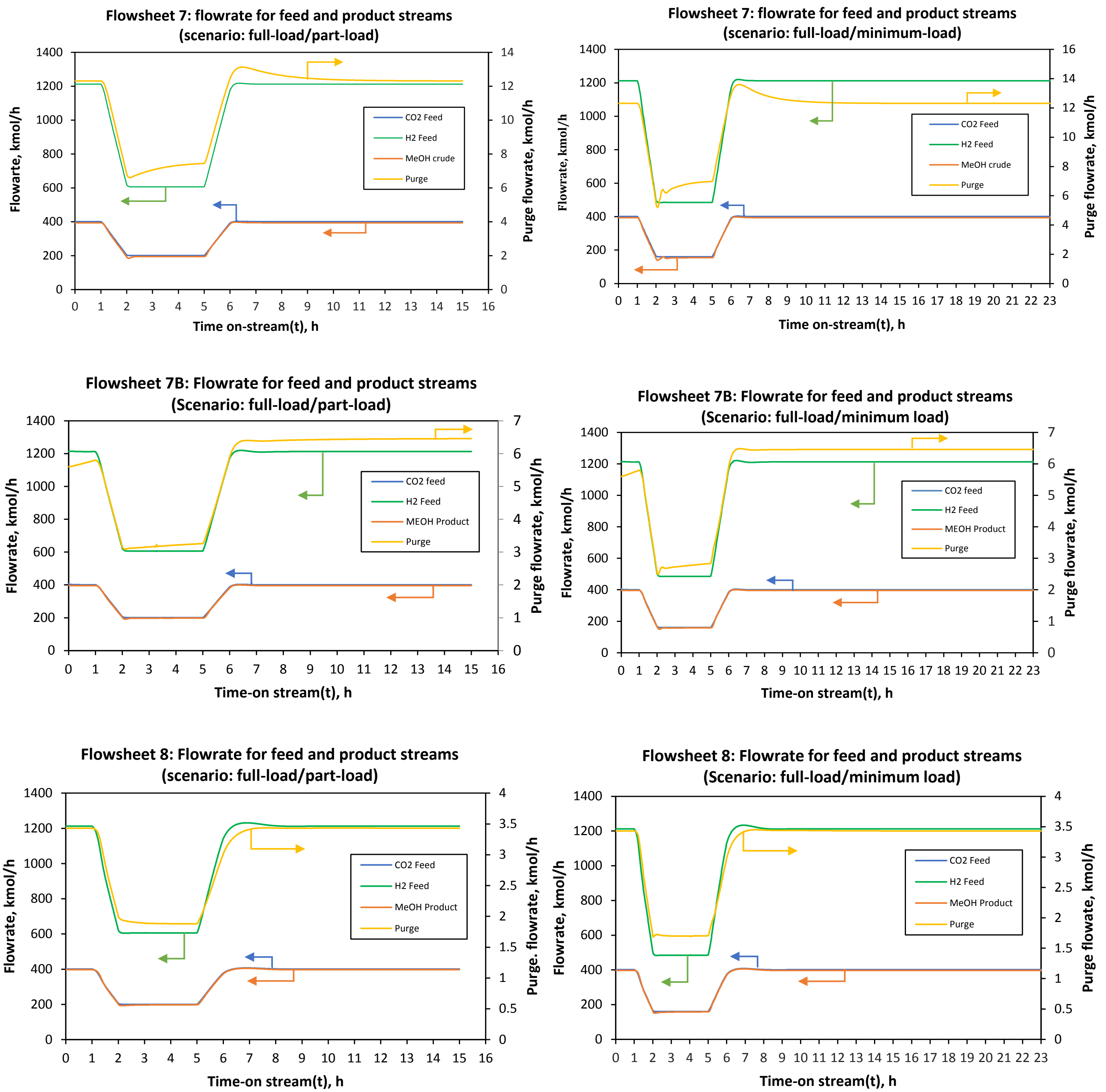

Figure 7: Shows the flowrate of the feed and the product streams when the load was changed from full-load (100%) to part-load (50%) and minimum load (40%). These results are for flowsheet 7, flowsheet 7B and flowsheet 8.

based flowsheets as depicted by Figure 8, the CO_2 hydrogenation had better load flexibility than the syngas-based flowsheet, even though the architecture of syngas-based flowsheet is similar to series-series flowsheet 8. However, operation at loads higher than nominal is possible (up to 110% for syngas-based flowsheet).

View Article Online
DOI: 10.1039/D4YA00433G

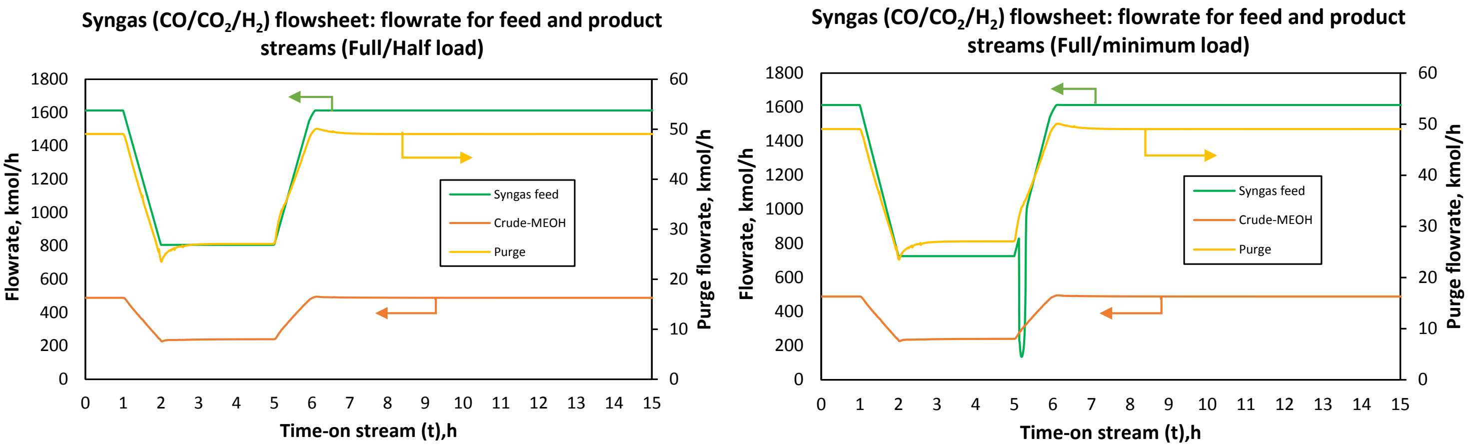

Figure 8: Shows the flowrate of the feed and the product streams when the load was changed from full-load (100%) to part-load (50%) and minimum load (45%) for co-electrolysis derived syngas to methanol.

Syngas-based flowsheet was also marred by the instabilities at minimum load, where undershoot were observed on the purge and syngas-feed when the load was ramped from the full-load to part-load and minimum loads to full-load. It also takes a while for the recycle splitter to maintain the split ratio and hence the observed drops in the purge stream. Any flowrate within the defined load range can be reached successfully, safely and without system shutdown when the control system is properly designed. The change in the adiabatic reactors exit temperatures with the load change was almost negligible for the CO_2 hydrogenation reaction. This is because as the feed flowrate is increased or decreased, the heat released is distributed across the reactor at higher feed flow, and the reverse water-gas shift reaction which gets more promoted at high residence time balances out the heat released at reduced flow. One would expect that with more methanol production more heat will be released in the reactors, but this is mitigated by these factors. In addition, the large recycle stream also causes the balancing effect providing the necessary temperature control and distribution. However, the potential effects of inaccuracies of the steady state kinetic model used to simulate the dynamic thermal profile must be investigated further. The current results shows that the storage capacity between the methanol synthesis reactors and the upstream process (electrolysis and CO_2 capture) can be reduced at-least to allow for operation in the defined load range (40-100%). Lower part-load are expected to be problematic more especially for the syngas-based process since the increase in residence time results into higher heat evolution inside the reactors creating possibility of hot-spot formation. However, the final decision on the design of the feed storage capacity(s) on the upstream of the first stage reactor will be detected by the economic feasibility of each point. The economics under dynamic conditions are not considered in this study. Regardless, it is clear from the analysis in this study that methanol synthesis via adiabatic reactors can operate over an extended load range comparable with adiabatic reactors for methanation reaction.[32]

View Article Online
DOI: 10.1039/D4YA00433G

3.3.2 Composition of the feed

The composition of the feed of the reactor varies with load change as depicted in Figure 9. For the parallel –series and series-series configuration, the CO_2, methanol, H_2O and CO molar content in the feed of all the three reactors decreases with decrease in load; interestingly following the same trend as the load change.

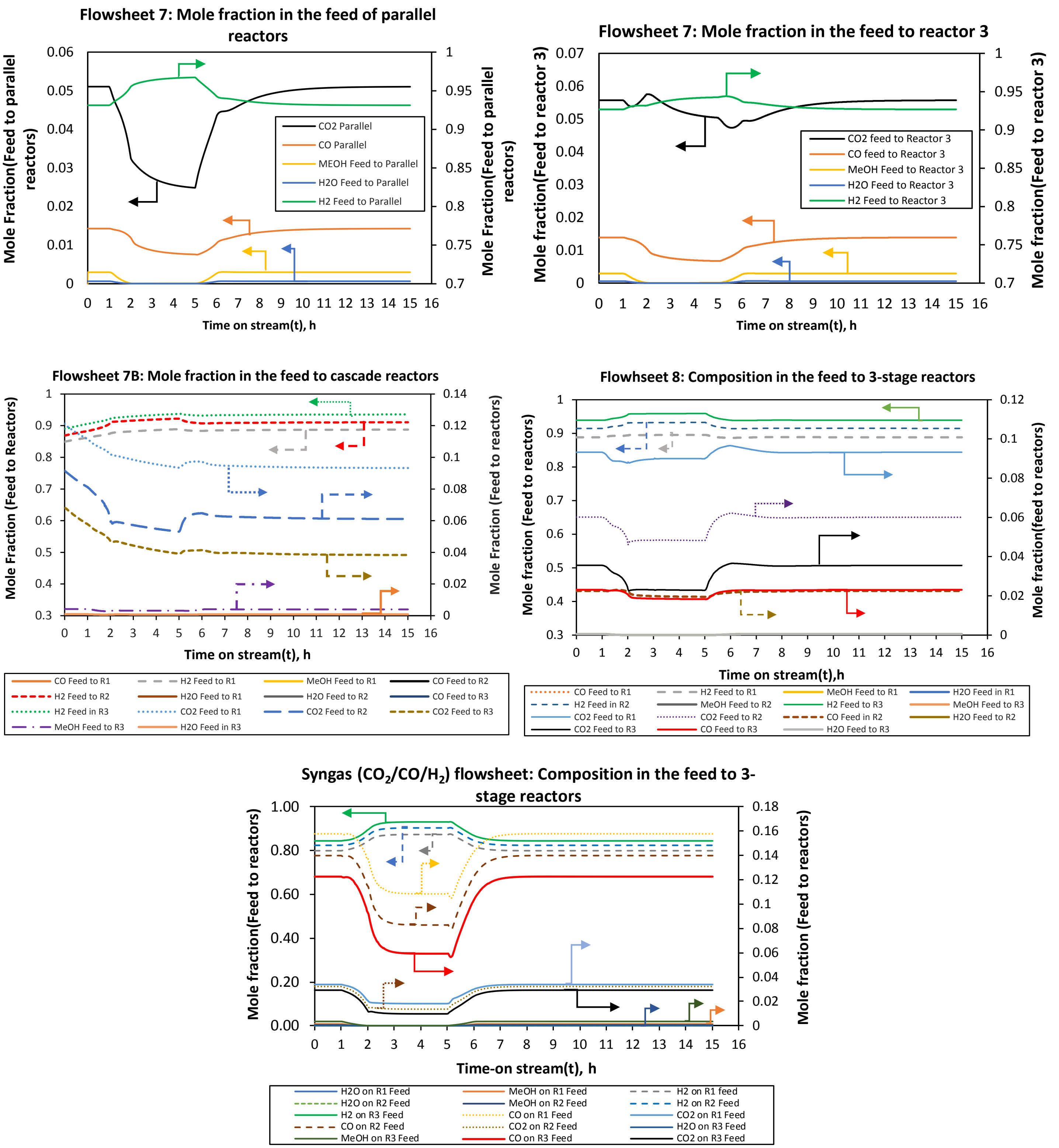

Figure 9: Shows the compositions of the feed streams to the reactors when the load was changed from full (100%) to half-load (50%).

View Article Online
DOI: 10.1039/D4YA00433G

However, the H_2 fraction in the reactor feed follow an opposite trend to load change. When load is reduced the H_2 content at all reactor inlet increases for all flowsheets. This is attributed to the fact that much of CO_2 gets converted during the load change such that, hydrogen is present in excess due to the recycle. High hydrogen content is seen in the last stage reactor. This is an interesting finding that hydrogen is in excess in the feed of the load flexible reactor during part-load. There is a slightly decreasing trend in the CO_2, methanol, H_2O and CO composition for Reactor 3 in flowsheet 7 and 7B, while flowsheet 8 shows a relatively similar decrease as with other reactors.

This shows that in flowsheet 8 the concentration inertia is eliminated across the process which is required to ensure flexible operation. It takes longer hours for the composition to achieve steady state, at-least for flowsheet 7 compared to flowsheet 8 and syngas-based flowsheet, as the load change, more especially for the last stage reactor in flowsheet 7. For flowsheet 8 and syngas-based flowsheet, the compositions need fewer hours to return to normal steady state after the disturbance. The parallel-series configuration (flowsheet 7) had pronounced overshoots and undershoots in the H_2 and CO_2 compositions.

3.3.3 Heat exchanger and compressor duties

Following the analysis of the Figure 10, the duties of the heat exchanger and the power of the compressors follow almost the same linear trend as the load change for all configurations. Considering the compressors duty for flowsheet 7, 7B and 8, there seems to be a similar linear decrease trend in the power of the recycle compressor(s) with changes in load from full (100%) to part-load (50%). For example, the compressor power for flowsheet 8 decreased from 236 kW at full-load to 131 kW at part-load, which is almost a 55% decrease. This can also be attributed to the high conversion at part-load (see Figure 12 for trend on conversion). On the other hand, for all the coolers in the considered systems, there is an increase in the cooling duties. This trend is similar to what Cui et al. observed and attributed to the quality of heat in the exit streams from the reactors, i.e., low grade heat of reactor effluent streams demands more cooling duty at part-load.[57] This is indeed the main energy loss for the methanol synthesis as has been discussed by other authors.[57] However, the impact of effective heat integration (that doesn't constraint flexibility but maximises the economics of the process) must be studied. It is expected that this may reduce the cooling requirements/demands for the methanol synthesis section. Again, the thermal inertia for the considered designs seems to be negligible. However, this remains to be confirmed. The heat exchanger duties are high for parallel-series flowsheet 7 compared to the series-series configuration and the lowest exchanger duties are found in the syngas-based configuration, more especially for the heaters. For all configurations no unfeasible heat exchanger duties (e.g., negative duties for the reactor preheaters) were observed.

View Article Online
DOI: 10.1039/D4YA00433G

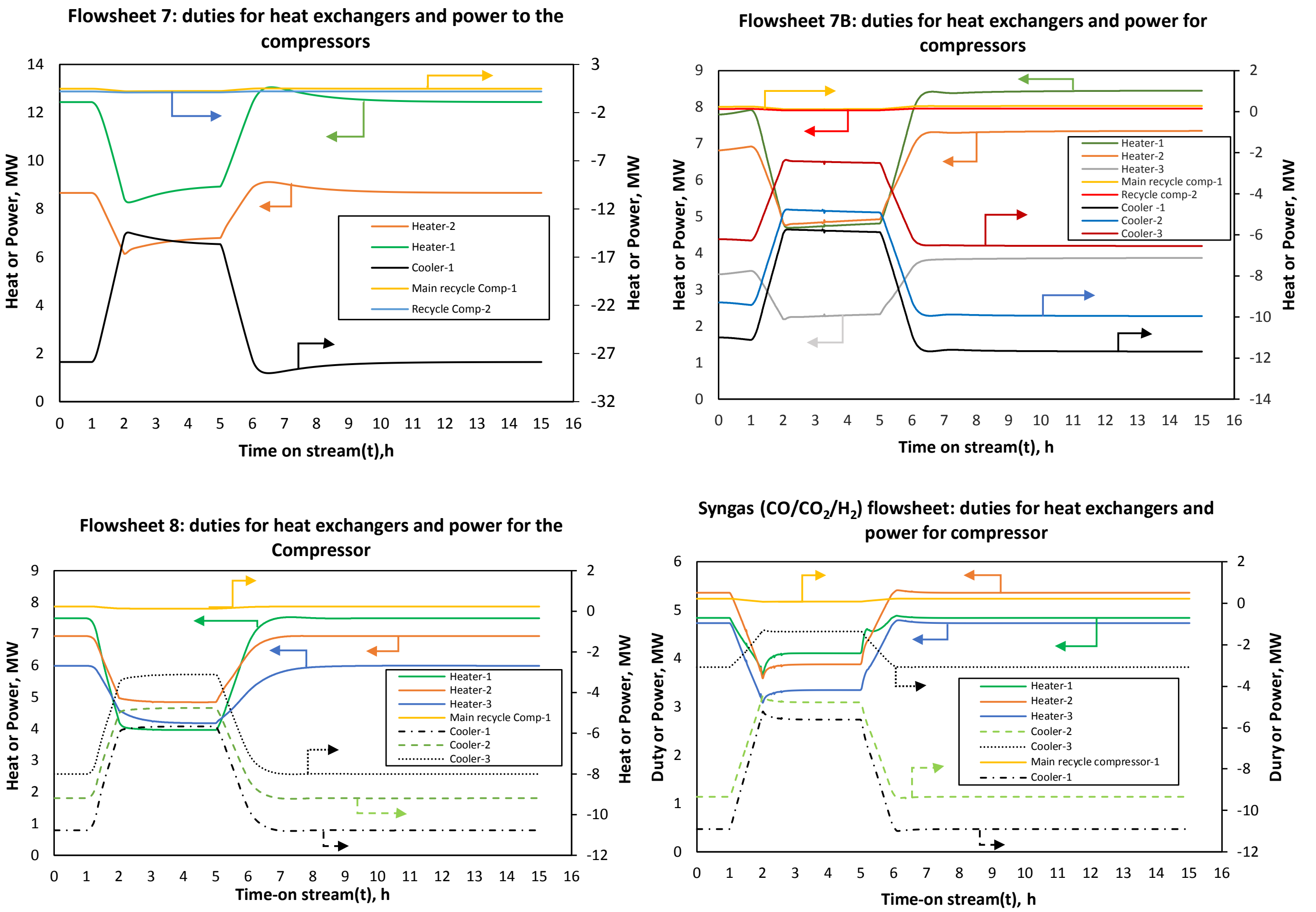

Figure 10: Shows the heat duties and power of the compressors to the reactors when the load was changed from full (100%) to half-load (50%).

3.3.4 Load dependent energy efficiency

To assess the load dependency of the energy efficiency of the three methanol synthesis configurations, a case without heat integration (no feed effluent heat exchange (FEHE) was simulated) while a case with minimum reactor outlet-feed heat integration (HI) (via hypothetically FEHE) was assumed. The trend depicted in Figure 11 shows a more pronounced decrease in energy efficiency with a decrease in the load for all the flowsheets when the heat integration via feed effluent (without FEHE) is not considered. For flowsheet 7 and 8, when the heat required to raise the temperature of the feed stream(s) to the reactor(s) feed was set to zero (assuming there could be heat integration using FEHE), the energy efficiency shows a very small variation from the full-load to all load levels (maximum, intermediate and minimum).

View Article Online
DOI: 10.1039/D4YA00433G

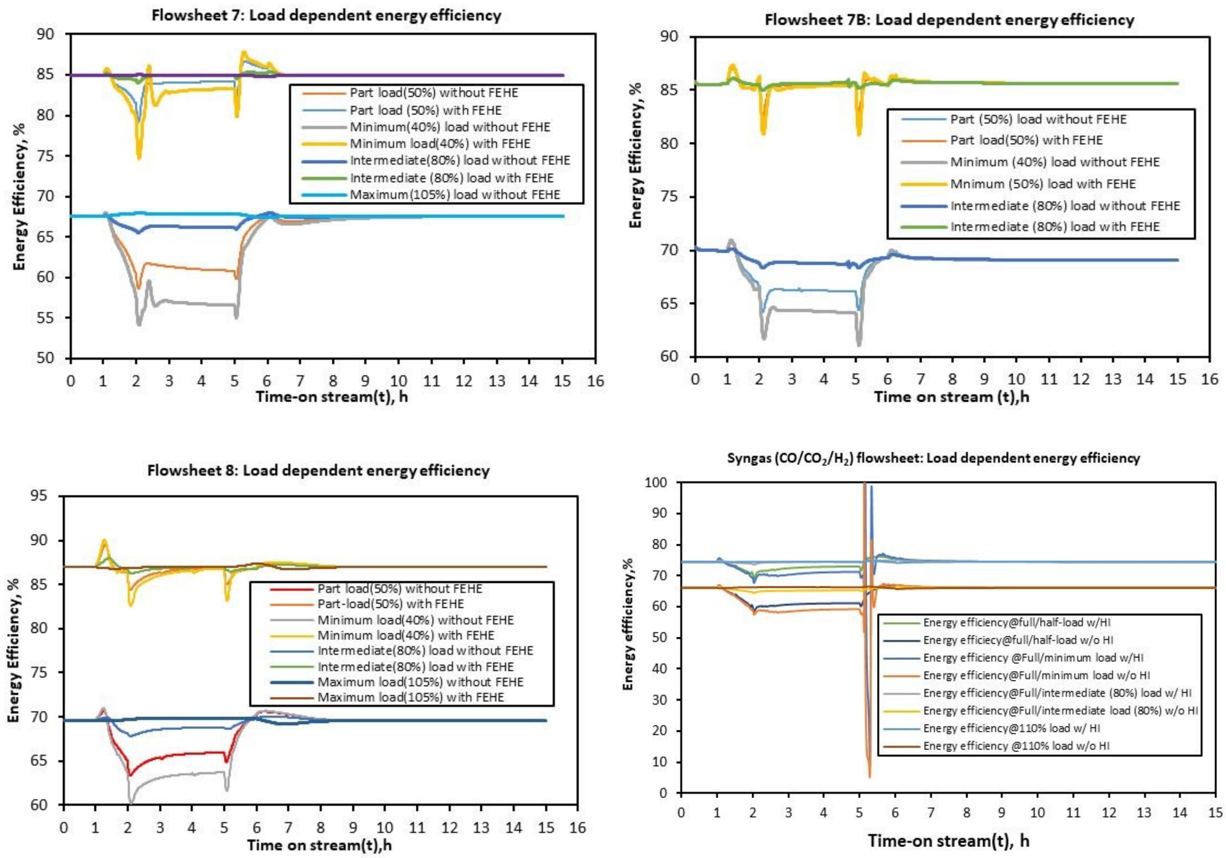

Figure 11: Shows the energy efficiency of the three configurations when the load was changed from full (105%) to half-load (50%), intermediate load (80%), and minimum load (40%). The ramp rate was kept constant at 60% load per hour.

For flowsheet 7B and 8, the energy efficiency is almost stable at steady state/full load energy efficiency when this minimum heat integration is considered. Although this heat integration is necessary to improve the energy efficiency, in real system it may induce the thermal oscillations due to tight coupling with the reactor. The assumption of a perfect (hypothetical) FEHE per reactor stage shows that enhancement of thermal dynamics is expected to improve the energy efficiency of the PtMeOH system. This will be more necessary and advantageous for the coupled methanol synthesis and upstream (electrolysis) at higher ramping rates since it is expected that the energy efficiency of the electrolysis will increase at low load and hence potentially increasing the overall energy efficiency of the coupled system.

The findings on energy efficiency trend for flowsheets 7 and 8 are similar to the recent finding that for a direct methanol synthesis reactor, dynamic modelling studies suggest that for part-load production capacity the energy efficiency does not decrease significantly as also deduced by Cui et al.[66] The energy efficiency of the methanol synthesis system in flowsheet 8 is higher than the other flowsheets. This effect is however

View Article Online
DOI: 10.1039/D4YA00433G

dampened by the electrolysis and distillation units when the overall integrated steady state simulation was considered in Figure 6 but it is expected to be more pronounced when effective heat integration is considered. For the syngas-based route, the load dependent energy efficiency is found to be lower than the other CO_2 hydrogenation systems, more especially when compared to flowsheet 8. The energy efficiency fluctuates significantly with decrease in the load. At loads above the nominal, the energy efficiency doesn't change significantly.

3.3.5 Single pass conversion

Conversion changes with load change. As illustrated in Figure 12, at part-load, the conversion is higher than the conversion at full-load for all the configurations. This is expected as the reduction in flowrate increases the residence time inside the reactor(s) and hence a positive step change in conversion result.

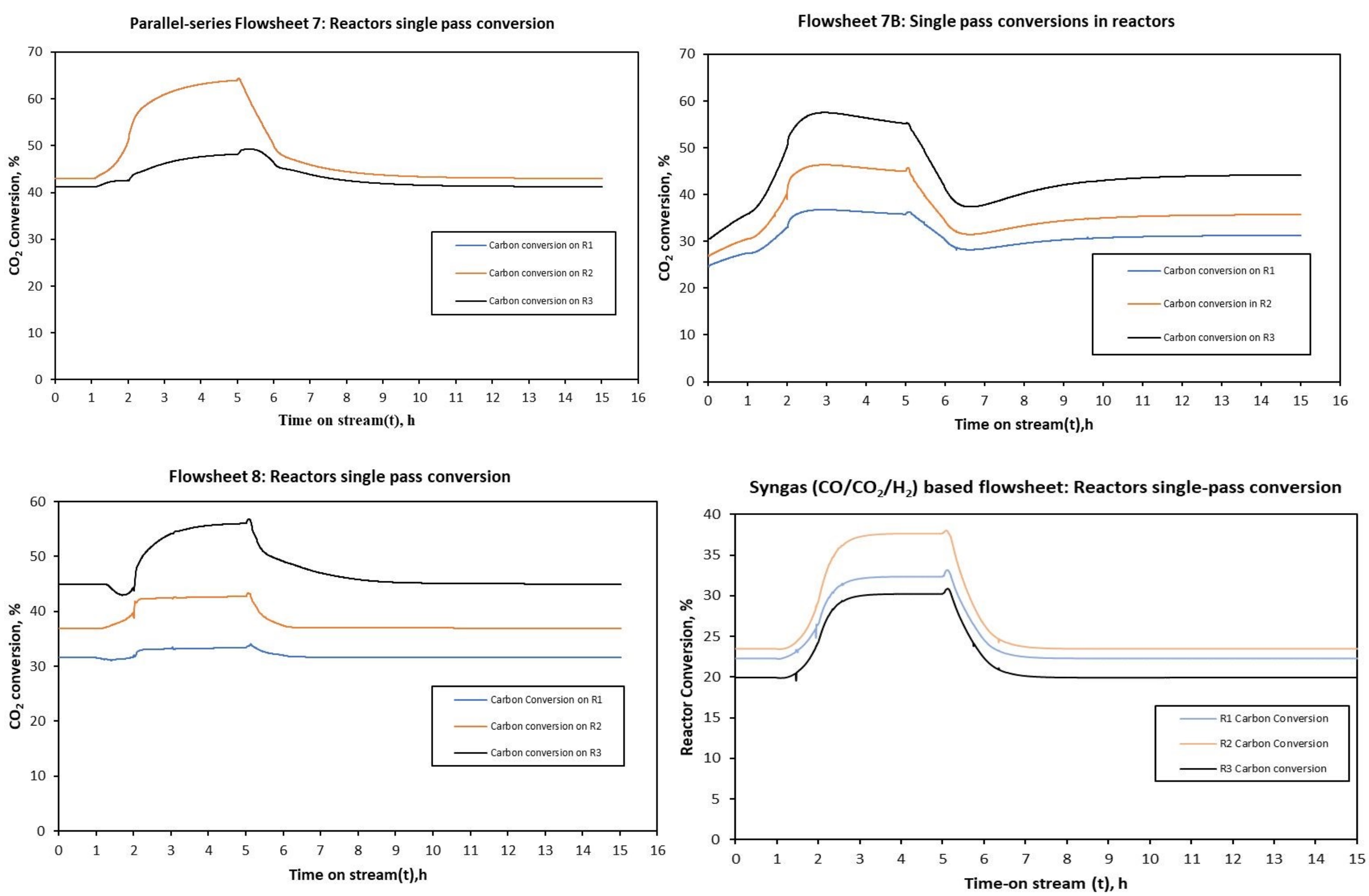

Figure 12: Shows the single pass reactor conversion for the three system configurations when the load was changed from full (105%) to half-load (50%).

The increase is slightly higher for parallel-series configuration in the parallel reactors (R1 and R2) due to their capacity and the fact that each feed to these reactors is further decreased, i.e., split by 50%, and thus

View Article Online
DOI: 10.1039/D4YA00433G

further rendering these reactors to operate at higher residence time than R3 and in contrast to R1, R2 and R3 of both configuration 7B, 8 and syngas-based flowsheet. For CO_2 hydrogenation-based flowsheet 7B and 8, conversion increases from first stage to last stage, with the last reactor stage having the highest single pass conversion compared to other reactors. However, the trend is opposite for the syngas-based reactor system. The second stage reactor has the highest conversion followed by the first stage and the last stage reactor.

3.4. Comparison of CO-rich route based on e-RWGS and Co-electrolysis-based process to the optimal CO_2 rich PtMeOH route.

Production of CO-rich syngas can be done by either using a RWGS reactor or SOEC via co-electrolysis. Co-electrolysis offers a resource-saving and regenerative alternative to conventional syngas production.[74-75] The syngas delivered by co-electrolysis can be easily varied by changing the ratio of CO_2/H_2O and it is in the range (H_2: CO at 1:1 to 3:1) desired for methanol synthesis. For fair comparison, the syngas feed coming from the electrolysis and e-RWGS was adjusted to 25.4/5.0/69.2% of $CO/CO_2/H_2$ with 0.4% H_2O to ensure similar methanol production rate as the CO_2 based process while maintaining the syngas ratio of 2.1. Co-electrolysis is currently investigated in the current second phase of the Kopernikus project "P2X" at the Energy Lab 2.0 at the Karlsruhe Institute of Technology (KIT).[74] Herein the energy efficiency of the co-electrolysis is compared to the optimal direct PtMeOH process and the process with e-RWGS. Recently, Haldor Topsoe has highlighted its interest in developing a renewable energy electrified reverse water gas shift reactor (e-RWGS).[76-77] The utilization of an e-RWGS reactor in methanol synthesis follows the CAMERE process relying on fire heated RWGS reactors.[76] Basini et al. evaluated the potential of this step but never compared it to other trending technologies such as co-electrolysis and CO_2-based PtMeOH overall processes under similar basis.[76] This section will discuss this comparison as it was modelled in this work. The SOEC-based co-electrolysis, steam electrolysis with and without e-RWGS are compared.

View Article Online
DOI: 10.1039/D4YA00433G

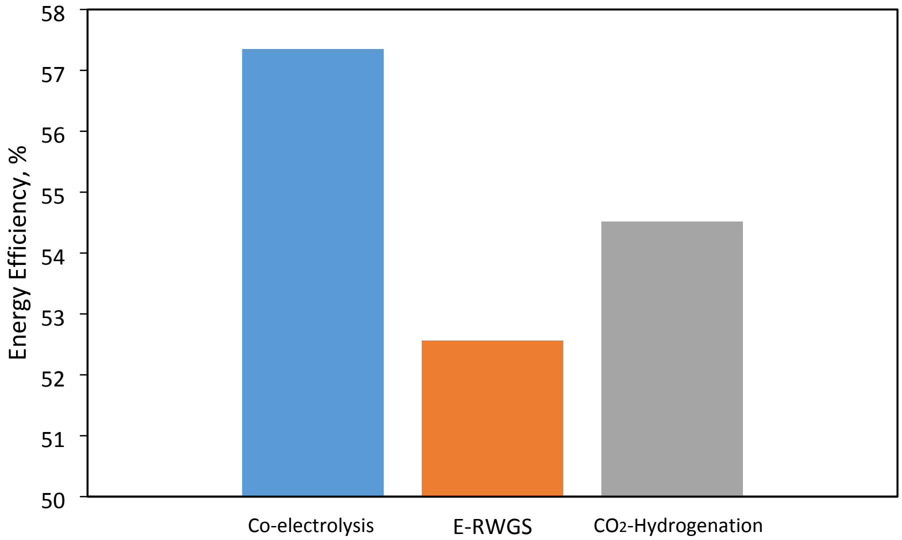

Figure 13: Energy efficiency comparison of co-electrolysis, e-RWGS, and CO_2 based power to methanol process.

Following from Figure 13, the co-electrolysis-based process has the highest energy efficiency followed by the SOEC steam electrolysis-based CO_2-hydrogenation and lastly the e-RWGS process. This is because the syngas produced from co-electrolysis in the SOEC has the higher heating value and the SOEC uses less heat under co-electrolysis compared to the steam electrolysis despite the co-electrolysis having higher electricity consumption.[50]

However, following from previous analysis, co-electrolysis may be flexible in terms of feed stock but for regions with largely fluctuating electricity up to very low loads, steam electrolysis-based methanol is recommended than the co-electrolysis-based process due to higher flexibility range of the CO_2 hydrogenation-based methanol process and the low power requirements for the SOEC steam electrolysis compared to SOEC-based on co-electrolysis mode as discussed in section 3.1. However, other factors may come into play such as the site-specific conditions, CO_2 emission reduction targets of the process and desired production rates.[78-79]

4. CONCLUSIONS

This work has compared twelve different SOEC-based power-to-methanol process configurations. The performance of the SOEC under steam- and co-electrolysis-based operation were first modelled and compared. The results shows that steam electrolysis uses less power than the co-electrolysis. However, the co-electrolysis based SOEC leads to the highest energy efficiency. Following from this, different adiabatic reactor configurations based on CO_2 hydrogenation were compared. Among these configurations, parallel-

View Article Online
DOI: 10.1039/D4YA00433G

parallel, parallel-series and series-series based configurations were integrated with the SOEC unit operating under steam electrolysis and compared considering the overall energy efficiency, conversion, production rate, and single pass conversion profiles. Three candidate process flowsheet featuring parallel-series and series-series based configuration were selected for further comparison. The selected parallel-series configurations (flowsheet 7) feature three reactors in which the first two are in parallel and in series with the third adiabatic reactor.

The selected promising series-series configuration (flowsheet 7B and 8) features three reactors in series with intermediate cooling and separation. Thereafter the sensitivity-based analysis or optimisation and heat integration are performed on the most promising flowsheets. The series-series configuration showed low utility requirements upon optimisation of the heat exchanger network. To further assess the potential of these configurations, dynamic simulation was performed using Aspen Dynamics to assess their flexibility in terms of load change and considering parameters such as load change flexibility range, time to steady state, composition changes, heat duty, power of the main units, load dependent energy efficiency, and single pass reactor conversion profile. The dynamic simulation also featured the comparison of CO_2 hydrogenation-based, and syngas (derived from co-electrolysis) based flowsheets. Time to reach steady state was shorter for parallel-series configuration compared to series-series configuration but the allowable load flexibility range (40-105%) is similar for all the three CO_2-based configurations. This indicates the potential to reduce the size of the intermediate product storage (e.g., H_2 storage) and allowing more flexible direct coupling of the electrolysis and methanol synthesis sections. The syngas-based flowsheet, although similar in architecture to the CO_2 hydrogenation-based flowsheet 8, cannot be ramped down to below 45% of the nominal load. Flowsheet 8 had the highest load dependent energy efficiency and reduced instabilities (undershoots and overshoots). Conversion increases with reduced load for all flowsheets. Overall, considering all factors, the series-based configuration with three adiabatic reactors in series is the most promising configuration. Multistage reactors offer the opportunity to promote flexibility by reducing the reactor overdesign, and allow for operating one reactor per time based on the available power supply and allowable idle period/downtime as may be set to prevent reactor damages and potential catalyst deactivation.

5. FUTURE WORK

Future work must conduct techno-economics of the flowsheets to better discriminate among the three candidate flowsheets for CO_2 hydrogenation. Furthermore, when the stoichiometric SOEC steam electrolysis-based integrated methanol synthesis is compared to co-electrolysis-based and to the e-RWGS-based configurations, the e-RWGS showed worse performance in terms of energy efficiency.

View Article Online
DOI: 10.1039/D4YA00433G

Although it has been demonstrated in this work that reactor configuration plays an important role in the performance of the dynamic power-to-methanol process, especially when the high efficiency electrolyser technology is used, more work is required to understand the dynamic operation strategies such as cold start-up, warm-standby, hot-standby and shutdown, and their effect on degradation and profitability of the process. For example, in the case of power-to-methanol operated with variable electricity, the reactor may need to be kept at stand-by mode to avoid condensation for example by recirculating the feed by means of bypassing the separator and shutting the purge thereby creating a batch system. Due to the enormous amount of energy required by the power-to-methanol via CO_2 hydrogenation, opportunities exist to further optimise the energy efficiency of the system with the intermediate product storage included. This must be assessed.

From the dynamic flexibility study conducted for the methanol synthesis section in this paper, it emanates that power to methanol will offer both flexibility and long-term energy storage in future markets. More data on hydrogen production are needed to further optimize the process. Future work should consider effects of perturbation of the feed conditions on the dynamics of the hot-spot temperature and methanol production from the low-cost adiabatic reactor as may be prevalent in the cases where variable power is used in power-to-methanol process. This includes variation of H_2-to-CO_2 ratio. The H_2-to-CO_2 ratio may be a major manipulable parameter in the case when renewable energy is used in power to methanol system. In this study, the CO_2 is assumed continuous and thus dynamic effects as well as the associated CO_2 storage are not considered. Future work should also consider the comparison of the heat integration potential when using water-cooled reactor which generates medium pressure steam against the adiabatic reactor in the case of power-to-methanol, in particular the steam utilization effect of coupling medium pressure steam to SOEC. This should also consider the thermal inertia in the catalyst and its effect on the process performance. In addition, because of different loads, the time co-ordination of heat recovery between various heat sources and sinks must be assessed as well as its associated economics and energy efficiency. This study considered constant pressure drop in the reactor. It would be necessary to consider variation in the pressure drop and effect of modifying the reactor design, e.g., internals, on the optimization of the proposed load flexible design. Future work should also consider integrating stochastic forecasting market model to the flexible process for advantageous response to different electricity prices and methanol selling prices. This can also be coupled with methanol fuel cells. In this work, simplified models were used to study the best configuration with minimal complexity and thus future work must consider more detailed (e.g. 2D) models including improved kinetic models (formulated with dynamic experimental conditions as well non-negligible heat and mass transports) for better optimisation of the load flexible reactor configuration while considering the sample electricity variation cycle and its corresponding H_2 and CO_2 production from the coupled electrolysis and capture processes, respectively. Other intensification methods such as structured reactors/catalysts must also be investigated and compared. It would also be interesting to understand the

View Article Online
DOI: 10.1039/D4YA00433G

significance of methanol reactor dynamics on the overall integrated efficiency of the PtMeOH process and quantify the benefit in terms of the overall plant availability.

DECLARATION OF COMPETING INTEREST

The authors declare that they have no known competing financial interests or personal relationships that could have appeared to influence the work reported on this paper.

ACKNOWLEDGEMENTS

This work was supported by the South African Department of Science and Innovation (DSI) for research activities under the HySA Infrastructure Centre of Competence (KP5 program, Project No. CNMH17X) and by the Council for Scientific and Industrial Research (CSIR) (Project Nos: C1GEN25, C8GOH26).

SUPPLEMENTARY MATERIAL

The Supporting Information is available free of charge on the attached supplementary material document.

Nomenclature

Symbol	Meaning (Unit)
AWE	Alkaline-water based electrolyser (–)
b_i	Logarithmic Arrhenius constants(–)
e-RWGS	Electrified Reverse Water Gas Shift Reactor
ΔG	Gibbs free energy (J mol^{-1})
ΔHr	Heat of reaction (kJ mol^{-1})
COR	Carbon oxide ratio (-)
$GHSV_0$	Gas hourly space velocity at nominal standard conditions (h^{-1})
GHSV	Gas hourly space velocity (NL.h^{-1}.gcat^{-1})
HEN	Heat Exhnager Network
LCOM	Levelised cost of methanol ($/tMEOH)
k_j	Reaction rate constant (–)
K_i	Adsorption constant (–)
M_{w_i}	Molecular weight (kg mol^{-1})
m_c	Mass of the catalyst (kg)
m_i	Mass of component (kg)
PteMeOH	Power to methanol
R	Ideal gas constant (J mol^{-1}K^{-1})

View Article Online
DOI: 10.1039/D4YA00433G

RKSMHV2	Redlich-Kwong Soave with Modified Huron-Vidal mixing rules
SN	Stoichiometric number (–)
T	Temperature (K)
SOEC	Solid oxide electrolyser (–)
ε	Fixed bed porosity (–)
ρ_{cat}	Catalyst density (kg m^{-3})

REFERENCES

1. Salmon N, Bañares-Alcántara R. Green ammonia as a spatial energy vector: a review. Sustainable Energy & Fuels. 2021.
2. Giannoulidis S, Venkataraman V, Woudstra T, Aravind PV. Methanol based Solid Oxide Reversible energy storage system–Does it make sense thermodynamically?. Applied Energy. 2020 Nov 15;278:115623.
3. Hank, C., Sternberg, A., Köppel, N., Holst, M., Smolinka, T., Schaadt, A., Hebling, C. and Henning, H.M., 2020. Energy efficiency and economic assessment of imported energy carriers based on renewable electricity. Sustainable Energy & Fuels, 4(5), pp.2256-2273.
4. Moioli, E., Mutschler, R. and Züttel, A., 2019. Renewable energy storage via CO2 and H2 conversion to methane and methanol: Assessment for small scale applications. Renewable and Sustainable Energy Reviews, 107, pp.497-506.
5. Chein RY, Chen WH, Ong HC, Show PL, Singh Y. Analysis of methanol synthesis using CO_2 hydrogenation and syngas produced from biogas-based reforming processes. Chemical Engineering Journal. 2021 Jun 15:130835.
6. Zheng Y, You S, Li X, Bindner HW, Münster M. Data-driven robust optimization for optimal scheduling of power to methanol. Energy Conversion and Management. 2022 Mar 15;256:115338.
7. González-Garay A, Frei MS, Al-Qahtani A, Mondelli C, Guillén-Gosálbez G, Pérez-Ramírez J. Plant-to-planet analysis of CO 2-based methanol processes. Energy & Environmental Science. 2019;12(12):3425-36.
8. Vázquez D, Guillén-Gosálbez G. Process design within planetary boundaries: Application to CO_2 based methanol production. Chemical Engineering Science. 2021 Jun 21:116891.
9. Luyben WL. Design and control of a methanol reactor/column process. Industrial & engineering chemistry research. 2010 Jul 7;49(13):6150-63.

View Article Online
DOI: 10.1039/D4YA00433G

10. Hankin A, Shah N. Process exploration and assessment for the production of methanol and dimethyl ether from carbon dioxide and water. Sustainable Energy & Fuels. 2017;1(7):1541-56.
11. Gogate MR. Methanol synthesis revisited: reaction mechanisms in CO/CO2 hydrogenation over Cu/ZnO and DFT analysis. Petroleum Science and Technology. 2019 Mar 4;37(5):603-10.
12. Bowker M. Methanol synthesis from CO_2 hydrogenation. ChemCatChem. 2019 Sep 5;11(17):4238.
13. Stefansson B. Power and CO_2 emissions to methanol. InPresentation, 2015 European methanol policy forum 2015 Oct.
14. Lee HW, Kim K, An J, Na J, Kim H, Lee H, Lee U. Toward the practical application of direct CO_2 hydrogenation technology for methanol production. International Journal of Energy Research.
15. Jiang X, Nie X, Guo X, Song C, Chen JG. Recent Advances in Carbon Dioxide Hydrogenation to Methanol via Heterogeneous Catalysis. Chemical Reviews. 2020 Feb 12.
16. Ruland H, Song H, Laudenschleger D, Stürmer S, Schmidt S, He J, Kähler K, Muhler M, Schlögl R. CO_2 hydrogenation with Cu/ZnO/Al2O3: A benchmark study. ChemCatChem. 2020 Apr 21.
17. Bos MJ, Kersten SR, Brilman DW. Wind power to methanol: Renewable methanol production using electricity, electrolysis of water and CO2 air capture. Applied Energy. 2020 Apr 15;264:114672.
18. Al-Kalbani H, Xuan J, García S, Wang H. Comparative energetic assessment of methanol production from CO_2: Chemical versus electrochemical process. Applied energy. 2016 Mar 1;165:1-3.
19. Pérez-Fortes M, Schöneberger JC, Boulamanti A, Tzimas E. Methanol synthesis using captured CO2 as raw material: Techno-economic and environmental assessment. Applied Energy. 2016 Jan 1;161:718-32.
20. Zhang H, Wang L, Pérez-Fortes M, Maréchal F, Desideri U. Techno-economic optimization of biomass-to-methanol with solid-oxide electrolyzer. Applied Energy. 2020 Jan 15;258:114071.
21. Rivera-Tinoco R, Farran M, Bouallou C, Auprêtre F, Valentin S, Millet P, Ngameni JR. Investigation of power-to-methanol processes coupling electrolytic hydrogen production and catalytic CO2 reduction. International Journal of Hydrogen Energy. 2016 Mar 2;41(8):4546-59.
22. Zhang H, Wang L, Maréchal F, Desideri U. Techno-economic optimization of CO2-to-methanol with solid-oxide electrolyzer. Energies. 2019 Jan;12(19):3742.
23. Alsuhaibani AS, Afzal S, Challiwala M, Elbashir NO, El-Halwagi MM. The impact of the development of catalyst and reaction system of the methanol synthesis stage on the overall profitability of the entire plant: A techno-economic study. Catalysis Today. 2020 Mar 1;343:191-8.

View Article Online
DOI: 10.1039/D4YA00433G

24. GhasemiKafrudi E, Samiee L, Pour ZM, Rostami T. Optimization of methanol production process from carbon dioxide hydrogenation in order to reduce recycle flow and energy consumption. Journal of Cleaner Production. 2022 Sep 23:134184.
25. Zondervan E, editor. Process Systems Engineering: For a Smooth Energy Transition. Walter de Gruyter GmbH & Co KG; 2022 Oct 3.
26. Voß JM, Duan T, Geitner C, Schluter S, Schulzke T. Operating behavior of a demonstration plant for methanol synthesis, Chemie Ingenieur Technik. 2022 Oct; 94(10): 1489-500.
27. Rodriguez Vallejo D. Promoting sustainability in chemical process design using process modelling, environmental assessment and decision making (Doctoral dissertation, Imperial College London).
28. Chiou HH, Lee CJ, Wen BS, Lin JX, Chen CL, Yu BY. Evaluation of alternative processes of methanol production from CO2: Design, optimization, control, techno-economic, and environmental analysis. Fuel. 2023 Jul 1;343:127856.
29. Zhou H, Wang J, Meng W, Wang K, Li G, Yang Y, Fan Z, Wang D, Ji D. Comparative investigation of CO2-to-methanol process using different CO2 capture technologies. Fuel. 2023 Apr 15;338:127359.
30. Bruns B, Herrmann F, Polyakova M, Grünewald M, Riese J. A systematic approach to define flexibility in chemical engineering. Journal of Advanced Manufacturing and Processing. 2020 Oct;2(4):e10063.
31. Chen C, Yang A. Power-to-methanol: The role of process flexibility in the integration of variable renewable energy into chemical production. Energy Conversion and Management. 2021 Jan 15;228:113673.
32. Mucci S, Mitsos A, Bongartz D. Power-to-X processes based on PEM water electrolyzers: A review of process integration and flexible operation. Computers & Chemical Engineering. 2023 Apr 14:108260.
33. Qi M, Vo DN, Yu H, Shu CM, Cui C, Liu Y, Park J, Moon I. Strategies for flexible operation of power-to-X processes coupled with renewables. Renewable and Sustainable Energy Reviews. 2023 Jun 1;179:113282.
34. Bruns B, Grünewald M, Riese J. Optimal design for flexible operation with multiple fluctuating input parameters. InComputer Aided Chemical Engineering 2022 Jan 1 (Vol. 51, pp. 859-864). Elsevier.
35. Qiu Y, Zhou B, Zang T, Zhou Y, Qi R, Lin J. Extended Load Flexibility of Industrial P2H Plants: A Process Constraint-Aware Scheduling Approach. arXiv preprint arXiv:2203.02991. 2022 Mar 6.

View Article Online
DOI: 10.1039/D4YA00433G

36. Lange H, Klose A, Lippmann W, Urbas L. Technical evaluation of the flexibility of water electrolysis systems to increase energy flexibility: A review. International Journal of Hydrogen Energy. 2023 Jan 31.

37. Li G, Gou Y, Ren R, Xu C, Qiao J, Sun W, Wang Z, Sun K. Realizing high-temperature steam electrolysis on tubular solid oxide electrolysis cells sufficing multiple and rapid start-up. Ceramics International. 2023 May 1;49(9):14101-8.

38. Zimmermann RT, Bremer J, Sundmacher K. Load-flexible fixed-bed reactors by multi-period design optimization. Chemical Engineering Journal. 2021 Jun 10:130771.

39. Salmon N, Bañares-Alcántara R. Impact of process flexibility and imperfect forecasting on the operation and design of Haber–Bosch green ammonia. RSC Sustainability. 2023.

40. Grossmann IE, Morari M. Operability, resiliency, and flexibility: Process design objectives for a changing world.

41. Rinaldi R, Visconti CG. Flexible operations of a multi-tubular reactor for methanol synthesis from biogas exploiting green hydrogen. Chemical Engineering Science. 2023 May 15;272:118611.

42. Svitnič T, Sundmacher K. Renewable methanol production: Optimization-based design, scheduling and waste-heat utilization with the FluxMax approach. Applied Energy. 2022 Nov 15;326:120017.

43. Siemens, 2024. Retrieved from: https://www.siemens-energy.com/global/en/home/products-services/product-offerings/hydrogen-solutions.html

44. Copenhagen Infrastructure Partners (CIP), 2021. Retrieved from: https://renewablesnow.com/news/cip-plans-power-to-x-plant-to-produce-green-methanol-764426/

45. Sánchez-Luján J, Molina-García Á, López-Cascales JJ. Optimal integration modeling of Co–Electrolysis in a power-to-liquid industrial process. International Journal of Hydrogen Energy. 2024 Jan 2;52:1202-19.

46. Samimi F, Feilizadeh M, Najibi SB, Arjmand M, Rahimpour MR. Carbon dioxide utilization in methanol synthesis plant: process modeling. Chemical Product and Process Modeling. 2020 Nov 2;1(ahead-of-print).

47. Rahimpour MR, Ghader S, Baniadam M, Fathi Kalajahi J. Incorporation of flexibility in the design of a methanol synthesis loop in the presence of catalyst deactivation. Chemical Engineering & Technology: Industrial Chemistry-Plant Equipment-Process Engineering-Biotechnology. 2003 Jun 4;26(6):672-8.

48. Léonard, G., Giulini, D. and Villarreal-Singer, D., 2016. Design and evaluation of a high-density energy storage route with CO2 re-use, water electrolysis and methanol synthesis. In Computer Aided Chemical Engineering (Vol. 38, pp. 1797-1802). Elsevier.

View Article Online
DOI: 10.1039/D4YA00433G

49. Kontogeorgis GM, Folas GK. The EoS/GE mixing rules for cubic equations of state. Thermodynamic Models for Industrial Applications: From Classical and Advanced Mixing Rules to Association Theories. John Wiley & Sons, Ltd, Chichester. 2010:159-93.
50. Patcharavorachot Y, Chatrattanawet N, Arpornwichanop A, Saebea D. Comparative energy, economic, and environmental analyses of power-to-gas systems integrating SOECs in steam-electrolysis and co-electrolysis and methanation. Thermal Science and Engineering Progress. 2023 May 11:101873.
51. Lonis, F. Design, modelling, evaluation and comparison of energy systems for the production and use of renewable methanol using recycled CO2. PhD thesis. University of Cagliari, 2020
52. Sunfire-Factsheet-HyLink-SOEC-20210303, https://www.sunfire.de/files/sunfire/images/content/Sunfire.de%20(neu)/Sunfire-Factsheet-HyLink-SOEC-20210303.pdf
53. Sunfire-Factsheet-SynLink-SOEC-20210303, https://www.sunfire.de/files/sunfire/images/content/Sunfire.de%20(neu)/Sunfire-Factsheet-SynLink-SOEC-20210303.pdf
54. Hansen JB, Christiansen N, Nielsen JU. Production of sustainable fuels by means of solid oxide electrolysis. ECS Transactions. 2011 Apr 25;35(1):2941.
55. Hossein Nami, Omid Babaie Rizvandi, Christodoulos Chatzichristodoulou, Peter Vang Hendriksen, Henrik Lund Frandsen,Techno-economic analysis of current and emerging electrolysis technologies for green hydrogen production,Energy Conversion and Management,Volume 269, 2022, 116162, ISSN 0196-8904, https://doi.org/10.1016/j.enconman.2022.116162.
56. Wang, L., Chen, M., Küngas, R., Lin, T.E., Diethelm, S. and Maréchal, F., 2019. Power-to-fuels via solid-oxide electrolyzer: Operating window and techno-economics. Renewable and Sustainable Energy Reviews, 110, pp.174-187.
57. Im-orb K, Visitdumrongkul N, Saebea D, Patcharavorachot Y, Arpornwichanop A. Flowsheet-based model and exergy analysis of solid oxide electrolysis cells for clean hydrogen production. Journal of Cleaner Production. 2018 Jan 1;170:1-3.
58. Jamshidi S, Sedaghat MH, Amini A, Rahimpour MR. CFD simulation and sensitivity analysis of an industrial packed bed methanol synthesis reactor. Chemical Engineering and Processing-Process Intensification. 2023 Jan 1;183:109244.
59. Lonis, F., Tola, V., Cascetta, M., Arena, S. and Cau, G., 2019, December. Performance evaluation of an integrated energy system for the production and use of renewable methanol via water electrolysis and CO2 hydrogenation. In AIP Conference Proceedings (Vol. 2191, No. 1, p. 020099). AIP Publishing LLC.

View Article Online
DOI: 10.1039/D4YA00433G

60. Lonis, F., Tola, V. and Cau, G., 2019. Renewable methanol production and use through reversible solid oxide cells and recycled CO2 hydrogenation. Fuel, 246, pp.500-515.
61. Kiss, A.A., Pragt, J.J., Vos, H.J., Bargeman, G. and De Groot, M.T., 2016. Novel efficient process for methanol synthesis by CO2 hydrogenation. Chemical engineering journal, 284, pp.260-269.
62. Cui, X. and Kær, S.K., 2020. A comparative study on three reactor types for methanol synthesis from syngas and CO2. Chemical Engineering Journal, p.124632.
63. Bussche KV, Froment GF. A steady-state kinetic model for methanol synthesis and the water gas shift reaction on a commercial Cu/ZnO/Al2O3Catalyst. Journal of Catalysis. 1996 Jun 1;161(1):1-0.
64. Van-Dal, É.S. and Bouallou, C., 2013. Design and simulation of a methanol production plant from CO2 hydrogenation. Journal of Cleaner Production, 57, pp.38-45.
65. Mignard D, Pritchard C. On the use of electrolytic hydrogen from variable renewable energies for the enhanced conversion of biomass to fuels. Chemical engineering research and design. 2008 May 1;86(5):473-87.
66. Cui X, Kær SK, Nielsen MP. Energy analysis and surrogate modeling for the green methanol production under dynamic operating conditions. Fuel. 2021 Sep.
67. Nestler, F., Schütze, A.R., Ouda, M., Hadrich, M.J., Schaadt, A., Bajohr, S., Kolb, T., 2020. Kinetic modelling of methanol synthesis over commercial catalysts: A critical assessment, Chem. Eng. J. 394, 124881. https://doi.org/10.1016/j.cej.2020.124881.
68. Slotboom, Y., Bos, M.J., Pieper, J., Vrieswijk, V., Likozar, B., Kersten, S.R., Brilman, D.W., 2020 Critical assessment of steady-state kinetic models for the synthesis of methanol over an industrial Cu/ZnO/Al2O3 catalyst, Chem. Eng. J. 389, 124181. https://doi.org/10.1016/j.cej.2020.124181.
69. de Oliveira Campos, B.L., Herrera Delgado, K., Pitter, S., Sauer, J., 2021b. Development of consistent kinetic models derived from a microkinetic model of the methanol synthesis, Ind. Eng. Chem. Res. 60 (42), 15074–15086. https://doi/full/10.1021/acs.iecr.1c02952.
70. Kiss, A.A., Pragt, J.J., van Iersel, M.M., Bargeman, G. and de Groot, M.T., 2013. Continuous process for the preparation of methanol by hydrogenation of carbon dioxide. WIPO Patent 2013144041.
71. Szima S, Cormos CC. Improving methanol synthesis from carbon-free H2 and captured CO2: a techno-economic and environmental evaluation. Journal of CO2 Utilization. 2018 Mar 1;24:555-63.
72. Parigi D, Giglio E, Soto A, Santarelli M. Power-to-fuels through carbon dioxide Re-Utilization and high-temperature electrolysis: A technical and economical comparison between synthetic methanol and methane. Journal of Cleaner Production. 2019 Jul 20;226:679-91.

View Article Online
DOI: 10.1039/D4YA00433G

73. Bansode A, Urakawa A. Towards full one-pass conversion of carbon dioxide to methanol and methanol-derived products. Journal of Catalysis. 2014 Jan 1;309:66-70.

74. de Hair B, Fantz U, Hecimovic A, Schulz A, Navarrete Munoz A, Klumpp M. Trend report technical chemistry 2021. News from chemistry. 2021 Jun; 69 (6): 52-9.

75. Zhan Z, Kobsiriphat W, Wilson JR, Pillai M, Kim I, Barnett SA. Syngas production by coelectrolysis of CO2/H2O: the basis for a renewable energy cycle. Energy & Fuels. 2009 Jun 18;23(6):3089-96.

76. Basini LE, Furesi F, Baumgärtl M, Mondelli N, Pauletto G. CO2 capture and utilization (CCU) by integrating water electrolysis, electrified reverse water gas shift (E-RWGS) and methanol synthesis. Journal of Cleaner Production. 2022 Dec 1;377:134280.

77. Thor Wismann S, Larsen KE, Mølgaard Mortensen P. Electrical Reverse Shift: Sustainable CO2 Valorization for Industrial Scale. Angewandte Chemie. 2022 Feb 14;134(8):e202109696.

78. Tsiklios C, Schneider S, Hermesmann M, Müller TE. Efficiency and Optimal Load Capacity of E-Fuel-Based Energy Storage Systems. Advances in Applied Energy. 2023 Apr 23:100140.

79. Ioannou I, D'Angelo SC, Galán-Martín Á, Pozo C, Pérez-Ramírez J, Guillén-Gosálbez G. Process modelling and life cycle assessment coupled with experimental work to shape the future sustainable production of chemicals and fuels. Reaction Chemistry & Engineering. 2021.

View Article Online
DOI: 10.1039/D4YA00433G

Data Availability Statement

The data that support the findings of this study are available from the corresponding author upon reasonable request.